RSC Advances

REVIEW

View Article Online
View Journal | View Issue

Cite this: *RSC Adv.*, 2026, **16**, 11874

Recent advances and challenges in advanced oxidation processes for degradation of nano- and microplastics in water: a critical review

Thi Ngoc Bao Dung,[a] Thi Thanh Huyen Nguyen,[bc] Quang Viet Ly,[d] Hui Lin Ong [e] and Hai Bang Truong *[fg]

This review consolidates recent advances in advanced oxidation processes (AOPs) for nanoplastic and microplastic (NMP) degradation, focusing on four major approaches: ozonation, photocatalysis, Fenton-based systems, and electrochemical oxidation. It critically examines how NMP characteristics, operational conditions, material design, and technological advancements influence system performance and degradation pathways. Ozonation of NMPs was enhanced through UV, ultrasound, or catalysts. Photocatalysis offers a sustainable route for degrading NMPs. Efforts such as heterojunction engineering, metal doping, and immobilization on various supports have improved activity and reusability, while multifunctional designs now allow simultaneous pollutant removal or hydrogen production. Fenton-based processes, particularly photo- and heterogeneous systems, extend operational flexibility and reduce iron leaching, but their NMP removal performance remains inconsistent, and emerging variants such as self-Fenton and bio-Fenton are still hampered by high energy requirements, slow kinetics, and scalability issues. Electrochemical oxidation of NMPs provides direct and indirect oxidative routes, with advances in electrode design, ranging from layered double hydroxides to doped-metal oxides, improving radical generation and durability. Hybrid electrochemical systems that combine sonication, oxidants, and membranes show further promise, though unresolved challenges include electrode leakage, reliance on indirect performance metrics, harsh operational conditions, and high energy use. Across all methods, integrated systems and advanced analytical tools are increasingly applied to enhance efficiency and clarify mechanisms. This review also highlights remaining knowledge gaps and proposes future directions, including the adoption of advanced analysis, standardized evaluation, and the development of scalable, cost-effective designs to ensure the safe and practical deployment of AOPs for NMP remediation.

Received 3rd December 2025
Accepted 20th February 2026

DOI: 10.1039/d5ra09364c

rsc.li/rsc-advances

1. Introduction

Plastics, synthetic polymers made mostly from fossil fuels, are widely used due to their low cost, durability, flexibility, and chemical resistance. These properties have driven continuous growth in production, reaching over 400 million metric tons annually by 2024.[1] Plastics are found in nearly all sectors, including packaging, construction, transport, agriculture, electronics, and personal care.[2] However, their widespread use has serious environmental consequences, as much of the waste escapes proper management. In 2019, macroplastics (larger than 0.5 mm) accounted for roughly 88% of plastic pollution, totaling around 20 million metric tons.[3] Plastic waste gradually breaks down into smaller particles, microplastics (less than 5 mm) and nanoplastics (typically under 100 nm), through the combined effects of sunlight, wind, mechanical abrasion, chemical exposure, hydrolysis, and water movement.[4] Surface water bodies are contaminated with nano- and microplastics (NMPs) through multiple pathways, including the degradation of plastic debris, discharge of treated and untreated domestic or industrial wastewater, atmospheric deposition, and surface runoff (Table 1).[5]

NMPs in aquatic environments vary in polymer type, size, and shape, with polymer composition often indicating their sources.[6] Frequently reported polymers include polyethylene (PE) and polypropylene (PP) from packaging materials,

[a]*Faculty of Environment and Labour Safety, Ton Duc Thang University, No. 19 Nguyen Huu Tho Street, Tan Hung Ward, Ho Chi Minh City, Vietnam. E-mail: thingocbaodung@tdtu.edu.vn*

[b]*Institute of Research and Development, Duy Tan University, Da Nang, Vietnam*

[c]*Faculty of Environmental and Chemical Engineering, Duy Tan University, Da Nang, Vietnam*

[d]*Smart Green Transformation Center (GREEN-X), VinUniversity, Vinhomes Ocean Park, Gia Lam, Hanoi 100000, Vietnam*

[e]*Faculty of Chemical Engineering & Technology, Universiti Malaysia Perlis (UniMAP), Jejawi, 02600 Arau, Perlis, Malaysia*

[f]*Optical Materials Research Group, Science and Technology Advanced Institute, Van Lang University, Ho Chi Minh City, Vietnam*

[g]*Faculty of Applied Technology, Van Lang School of Technology, Van Lang University, Ho Chi Minh City, Vietnam. E-mail: truonghaibang@vlu.edu.vn*

Table 1 List of abbreviations used in the study

Abbreviation	Meaning
AOPs	Advanced oxidation processes
EC	Electrochemical
FE-SEM	Field emission scanning electron microscopy
FT-IR	Fourier transform infrared spectroscopy
GPC	Gel permeation chromatography
^{1}H NMR	Hydrogen-1 nuclear magnetic resonance
HPLC	High-performance liquid chromatography
MOF	Metal–organic framework
NIR	Near-infrared spectroscopy
NHE	Normal hydrogen electrode
NMPs	Nano- and microplastics
MPs	Microplastics
NPs	Nanoplastics
OM	Optical microscopy
PAN	Polyacrylonitrile
PE	Polyethylene
PET	Polyethylene terephthalate
PMS	Peroxymonosulfate
PP	Polypropylene
PS	Polystyrene
PVC	Polyvinyl chloride
SCE	Saturated calomel electrode
SHE	Standard hydrogen electrode
TOC	Total organic carbon
UV	Ultraviolet

polystyrene (PS) from insulation and disposable products, polyamide (PA) from fishing gear and textiles, polyacrylates from paints and coatings, polyvinyl chloride (PVC) from pipes and flooring, and polyurethane (PU) from foams. This diversity mirrors the extensive use of plastics across domestic, industrial, and commercial sectors. NMP morphology is largely determined by origin and degradation processes.[7,8] Fragments arise from the breakdown of larger plastic items, films from thin materials such as bags and agricultural plastics, and fibers primarily from the washing of synthetic textiles. Spherical microbeads from personal care products and foam particles derived from expanded polystyrene are also commonly observed. Detection becomes increasingly difficult with decreasing particle size, resulting in comparatively limited studies on nanoplastics. NMPs are now recognized as persistent and bioavailable pollutants posing substantial ecological risks.[9] They accumulate in aquatic systems and are taken up by organisms through ingestion, contaminated prey, filter feeding, and sediment contact.[10] Nanoplastics can penetrate cellular membranes and accumulate in tissues, with documented physiological and behavioral effects across multiple trophic levels, including phytoplankton, zooplankton, corals, fish, sea turtles, and seabirds. Emerging evidence also indicates potential human health risks through the consumption of contaminated seafood and drinking water.[11] NMPs may act as vectors for toxic chemicals, heavy metals, and pathogens, potentially inducing oxidative stress, inflammation, immune dysfunction, and endocrine disruption. Their detection in human blood, lungs, and placental tissues further highlights concerns regarding long-term health impacts. Accurate detection of NMPs in water remains challenging due to matrix interference. Common pre-treatment steps include sieving, drying, chemical digestion, density separation, and filtration to isolate particles.[12] Stereomicroscopy coupled with FTIR is widely used for larger particles,[13] whereas micro-FTIR and Raman spectroscopy extend detection limits to approximately 50 μm and 20 μm, respectively, and laser direct infrared (LDIR) spectroscopy enables automated analysis. For mass-based quantification, TD-GC/MS and Py-GC/MS are effective tools.[14] However, nanoplastic identification remains technically demanding and often requires advanced approaches such as AFM-IR, surface-enhanced Raman scattering (SERS), confocal Raman microscopy (CRM), and Py-GC/MS to achieve reliable detection in complex matrices.[15]

To evaluate the research fields of relating to NMPs, we use VOSviewer[16] to construct networks of scientific publications containing terms "microplastics" or "nanoplastics" from the Lens' bibliographic database. 46 846 publications were found containg "microplastics" in title or keywords, which was nearly 6 times higher than that for "nanoplastics", showing partially difficulties in the study of nanoplastics or nanoplastics in a more recent concern. From the total 49 762 scholarly works, 4214 terms were determined that occurs in at least 5 different studies. 600 terms with the greatest total link strength were selected for the network visualization (Fig. S1a). Noticeably, the terms relating to detection, monitoring and quantification occurred 7745 times, much higher than the occurrence of the terms relating to treatment, removal or degradation (3810 times). The publication disparity suggests that the field is still heavily focused on understanding and monitoring the microplastic pollution crisis, while removal technologies are lagging due to technical, regulatory, and economic challenges.

Detection and monitoring of NMPs are essential for understanding their occurrence, distribution, and potential impacts on human and environmental health. However, due to the increasing concern over their potential toxicological risks, recent research has shifted significant focus toward developing and evaluating effective removal strategies. This growing interest reflects the urgent need not only to track NMP contamination but also to mitigate their presence in water systems through reliable treatment technologies. Adsorption is the most widely studied method for NMP removal in water purification, accounting for approximately 52% of related publications (Fig. S1b). Adsorption is simple, cost-effective, and efficient, relying on interactions like hydrogen bonding, hydrophobic forces, and electrostatic attraction. Its effectiveness depends on NMP properties, adsorbent type, pH, temperature, and contact time.[17] A wide range of adsorbents, including biochar, activated carbon, aerogels, nanoparticles, and biopolymers, have been tested for MP removal.[18] Coagulation/flocculation is widely used to remove NMPs in drinking water treatment, with aluminum salts generally outperforming iron.[19] Removal efficiency depends on particle size, shape, polymer type, coagulant dose, and process conditions. Fibrous NMPs are more easily removed, while smaller or low-density particles like PE are less effectively captured. Natural organics and salts can affect performance, and overdosing coagulants may increase

costs and operational issues.[20] Sand filtration effectively removes large microplastics (≥300 μm), especially with low-porosity or dual-media filters, but performs poorly for particles <50 μm.[21] Removal depends on NMPs size, shape, and filter properties, with fibers removed more efficiently. Membrane filtration offers higher precision *via* size exclusion, with UF and smaller-pore membranes blocking most NMPs.[22,23] However, membrane wear and particle interactions may reduce efficiency, and some studies suggest polymer membranes might release NMPs under stress. Separation-based methods are less effective for small NMPs, often generate secondary waste, and may suffer from membrane fouling or clogging. Chemical-based processes like coagulation produce sludge and can alter water chemistry. Besides the separation-based processes above, degradation-based methods chemically or biologically break down NMPs into less harmful substances or mineralized NMPs to gases. Biodegradation involves microbes or enzymes (*e.g.*, *Pseudomonas*, *PETase*) that target specific plastics, though the process is often slow and material-specific.[24] Thermal and thermochemical methods such as pyrolysis, gasification, and incineration decompose NMPs at high temperatures, converting them to fuel, syngas, or ash, but can be energy-intensive and require emission control.[25] Advanced oxidation processes (AOPs) use reactive species like hydroxyl and sulfate radicals, *via* photocatalysis, Fenton reactions, ozonation, or persulfate activation, to cleave polymer chains into CO_2, water, and smaller organics.[26] AOPs contributed 28% of publications relating to the removal and degradation of NMPs (Fig. S1b). AOPs can achieve complete mineralization of NMPs into harmless end products like CO_2 and H_2O,[27] with faster reaction rates than biodegradation. Unlike thermal methods such as pyrolysis or incineration, AOPs often operate under ambient conditions, making them more energy efficient. They are also effective across a wide range of plastic types and do not rely on specific microbial activity, making them more versatile and stable under varying environmental conditions.[28] Additionally, AOPs can be integrated into existing treatment systems and typically produce minimal secondary waste when properly optimized.

Given the rising environmental and health concerns associated with NMPs, there is an urgent need for effective and sustainable treatment technologies. Among the available degradation-based strategies, AOPs have shown significant promise, owing to their capacity to convert NMPs into harmless end products, rapid reaction rates, and compatibility with relatively mild operating conditions. Nonetheless, current research on AOP applications for NMP remediation remains fragmented, with considerable variability in experimental approaches, targeted polymer types, and reported outcomes. This review consolidates and evaluates recent progress in AOP-driven NMP degradation technologies (Fig. 1), focusing on four key methods: (1) ozonation, (2) photocatalysis, (3) Fenton-based processes, and (4) electrochemical AOPs. It provides a critical

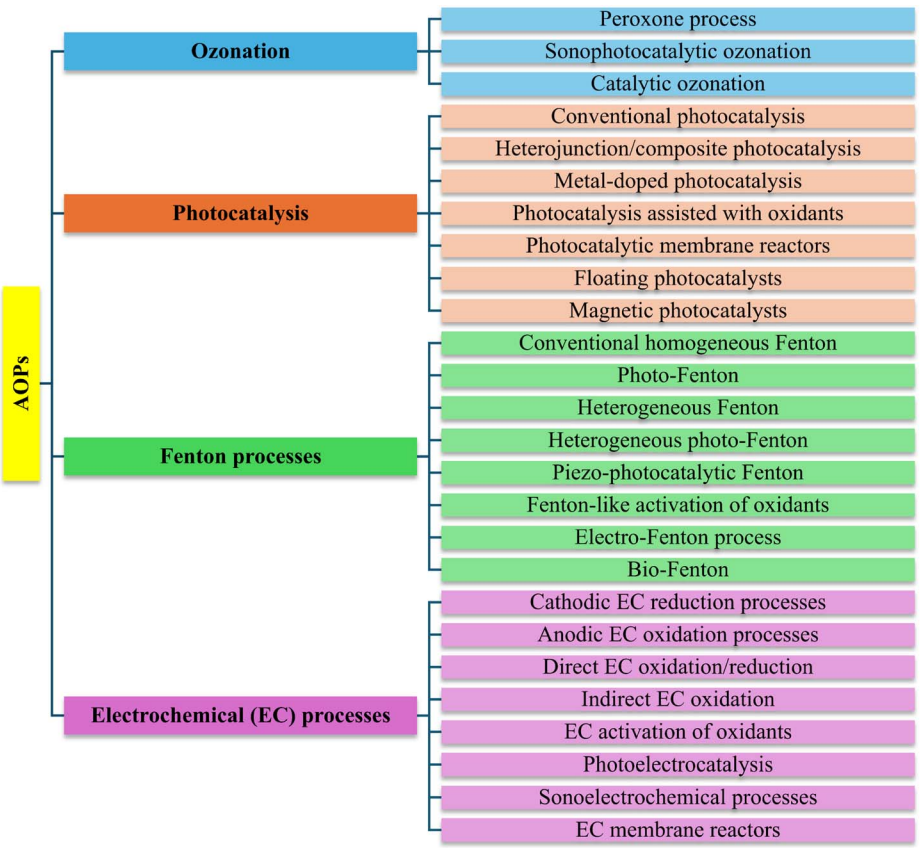

Fig. 1 Categorization of advanced oxidation processes reviewed in this study.

analysis of target NMP characteristics (*e.g.*, size, morphology, composition), operational parameters, removal mechanisms, technological advancements, and existing challenges. Furthermore, this work highlights key knowledge gaps and offers recommendations to inform future research and practical implementation.

2. Ozonation treatment of NMPs

Ozonation is an advanced oxidation process widely employed in both wastewater and drinking water treatment facilities for the removal of pollutants and microbial disinfection. Ozone (O_3) is a strong oxidizing agent, with a standard oxidation potential of approximately 2.07 V, capable of directly oxidizing hydrocarbon polymers to form peroxy radicals and carbonyl compounds (eqn (1) and (2)).[29] In aqueous environments, O_3 can also generate highly reactive species such as hydroxyl radicals (eqn (3)–(6)), which play a key role in the degradation of contaminants.[30] These reactive species can attack a broad spectrum of organic pollutants commonly found in contaminated surface water and groundwater.

$$R\text{–}CH + O_3 \rightarrow R\text{–}COO^{\bullet} + {}^{\bullet}OH \quad (1)$$

$$2R\text{–}COO^{\bullet} \rightarrow R\text{–}C{=}O + R\text{–}C\text{–}OH + O_2 \quad (2)$$

$$O_3 + OH^- \rightarrow HO_2^- + O_2 \quad (3)$$

$$O_3 + HO_2^- \rightarrow HO_2^{\bullet} + {}^{\bullet}O_3^- \quad (4)$$

$${}^{\bullet}O_3^- + H^+ \rightarrow HO_3^{\bullet} \quad (5)$$

$$HO_3^{\bullet} \rightarrow {}^{\bullet}OH + O_2 \quad (6)$$

The effectiveness of ozone in breaking down polymer-based particles such as microplastics in drinking water systems remains insufficiently studied. Some reports have indicated that ozonation primarily oxidizes the surface of NMPs without inducing significant degradation or fragmentation.[29,31] For instance, in the ozonation of polyethylene MPs, analyses using FT-IR and XPS revealed increased carbonyl and hydroxyl indices, higher O/C ratios, and surface oxidation occurring mainly in the amorphous regions of the particles. However, no substantial breakdown of C–C bonds or alterations in the

Table 2 Overview of the recent studies using ozone-based processes for MNP treatment

Ozone-based system	NMPs (concentration, shape, size)	Operational conditions	Removal efficiency and degradation rate (quantification method)	References
O_3	Polyethylene MPs (1% w/v)	O_3 dose: 7 mg L^{-1} Time: 3 h	Surface oxidation (no fragmentation)	29
O_3	Polyacrylonitrile core-polystyrene shell NPs (1.7 mg L^{-1}, ~215 nm)	O_3 dose: 5 mg L^{-1} Time: 45 min pH 6.8	Surface oxidation (no fragmentation)	31
O_3	Microplastics (164 MPs L^{-1}, microbead, fragment, fiber, & sheet)	O_3 dose: 12.6 mg L^{-1} Time: 1 min	80% degradation (OM)	33
O_3	Polystyrene NPs (2.5 μg L^{-1}, sphere, 80–300 nm)	O_3 dose: 4.1 mg L^{-1} Time: 6 h pH 6.4	96.3% degradation (GPC) 42.7% mineralization (TOC)	34
O_3	Microplastics (2100–6400 MPs L^{-1}; PE, PP, PS, PA, PET, PVC, fiber & fragment, 20–500 μm)	O_3 dose: 12 g h^{-1} Time: 5 h	45% degradation (OM) $k = 0.41 \pm 0.06$ h^{-1}	28
O_3	Polyethylene MPs (50 MPs L^{-1}, fiber, 0.2–5 mm)	O_3 dose: 10 mg L^{-1} Time: 75 min pH 5	92% degradation (OM)	32
O_3 + ultrasonication + UV light	Polyethylene MPs (granule, 4 mm)	O_3 dose: 5 g min^{-1} 28 kHz US, 9 W UV Time: 8h	100% mineralization (TOC)	35
O_3 + H_2O_2	Polyethylene MPs (0.05 g L^{-1}, fragment, 40–48 μm)	O_3 dose: 11.5 mg L^{-1} H_2O_2 dose: 20 mM Time: 8 h	32.6% mineralization	36
CeO_x@MnO_x/O_3	Polystyrene NPs (2 mg L^{-1}, sphere, 80–300 nm)	O_3 dose: 2.8 mg L^{-1} Catalyst dose: 5 mg L^{-1} Time: 50 min	96.7% degradation (GPC)	37
Co^{2+}/O_3	Polystyrene NPs (20 mg L^{-1})	O_3 dose: 5 mg min^{-1} Co^{2+} dose: 1 mM pH 3 Time: 2 h	70% mineralization (TOC)	38
α-FeOOH/O_3	Polyethylene MPs (1 g L^{-1}, 40–48 μm)	O_3 dose: 11.5 mg L^{-1} α-FeOOH dose: 20 mM pH 8 Time: 8 h	Yield of inorganic carbon (CO_2 production): 5.75 mg L^{-1} h^{-1}	39

crystalline regions were observed, likely due to the limited penetration of ozone into these more structured domains.[29] Reaction time played a more critical role than ozone concentration in determining the extent of oxidation. Similarly, Pulido-Reyes *et al.* reported that ozonation did not lead to fragmentation or agglomeration of NPs but did increase the negativity of the surface charge, likely because of carboxylic group formation during surface oxidation.[31]

In contrast, several studies have demonstrated the successful degradation and mineralization of NMPs through ozonation (Table 2). For instance, Topkaya *et al.* (2025) investigated the application of ozone oxidation for removing microplastics from cooling wastewater produced by a polyethylene stretch film manufacturing facility. Under optimized conditions, ozone concentration of 10 mg L^{-1}, pH 5, and a reaction time of 75 minutes, they achieved a removal efficiency of up to 92%.[32] According to Solís-Balbín *et al.*, variations in the initial concentration of microplastics had little impact on the overall removal efficiency. Additionally, fiber-shaped microplastics exhibited higher average removal rates compared to fragments.[28] Despite such promising results, identifying the most effective ozonation system across studies remains challenging due to significant variations in the characteristics of target NMPs, operational conditions, and quantification techniques employed. Hidayaturrahman and Lee examined ozonation treatment in a tertiary wastewater treatment plant, where the influent water contained 164 MPs per liter, including microbeads, fragments, fibers, and sheets.[33] With an ozone dose of 12.6 mg L^{-1}, approximately 80% of MPs were degraded within just one minute. Extremely high removal reported within very short reaction times should be interpreted cautiously, as such results may limit mechanistic understanding. In contrast, Solís-Balbín *et al.* (2023) reported a 45% MP degradation after 5 hours of ozonation at an ozone input rate of 12 g h^{-1}.[28] Ozonation in 5 hours at a O_3 concentration of 12 g h^{-1} can degrade 45% of MPs. However, their study involved a more complex mixture of polymer types (PE, PP, PS, PA, PET, and PVC), morphologies (fibers and fragments), sizes (20–500 μm), and much higher MP concentrations (2000–6500 MPs L^{-1}). Although both studies relied on visual microscopy for MP quantification, the substantial differences in MP properties and experimental conditions, particularly initial concentrations, make it nearly impossible to draw a direct comparison or determine which ozonation system was more effective.

Beyond quantification, several studies have investigated the degradation pathways of NMPs during ozonation. Pattanateeradetch *et al.* proposed a mechanism for PE degradation based on XRD, Raman, and XPS analyses. Ozonation first forms unstable ozonoids, which then break down C=C bonds, resulting in intermediate products enriched with oxygen-containing functional groups.[35] Li *et al.* investigated the degradation of polystyrene NPs using ozonation.[34] The presence of phenyl rings in the polystyrene structure renders these particles chemically reactive, as they are prone to attack by ozone and molecular oxygen, leading to aromatic ring cleavage. Nevertheless, the removal of relatively low NP concentrations (2.5 μg L^{-1}) required extended treatment times of up to 4 hours, and the extent of mineralization remained limited, with less than 50% of the carbon fully oxidized. In another investigation, Hu *et al.* applied two-dimensional correlation spectroscopy with FTIR-ATR spectra to monitor the chemical degradation of PE under H_2O_2/O_3 treatment. Hydroxyl radicals ($^{\bullet}OH$) rapidly formed and primarily attacked $-CH_2-$ groups, creating unstable alcohols that reacted further to form carbonyl compounds. Ozone also contributed by forming epoxides that caused chain scission and introduced various oxygen-containing groups, including C–O, C–OH, C=O, and C–O–C. The functional group transformation followed a progression from C–H to C=O, then to C–O and related species.

To gain a deeper understanding of NMP removal mechanisms during ozonation, it is important to consider not only chemical oxidation but also physical processes. Solís-Balbín *et al.* emphasized that physical entrainment plays a significant role, where the velocity of the ozone gas stream exceeds the particles' settling rate, further facilitating the release of NMPs, particularly fiber-shaped ones, into the gas phase[28] (Fig. 2a). In open systems, hydrophobic MPs can attach to rising air bubbles introduced through a diffuser. As these bubbles reach the surface, they burst, releasing the attached NMPs into the atmosphere *via* convective forces, a phenomenon known as bubble bursting.

To enhance the efficiency of NMP removal, various technologies have been integrated with ozonation. Strategies to enhance ozonation efficiency include the use of H_2O_2/O_3,[36] ultrasound/UV irradiation (US/UV),[35] catalytic ozonation with CeOx@MnOx,[37] metal ion-assisted ozonation using Co^{2+},[38] and combined catalytic ozonation with H_2O_2.[39] In a recent study, Pattanateeradetch *et al.* improved ozonation performance by applying ultrasonic irradiation (28 kHz) and UV light (9 W) during the treatment of PE in water.[35] The proposed degradation mechanism in US/UV/O_3 system is primarily driven by indirect ozonation, where ozone reacts with water under UV exposure to generate $^{\bullet}OH$ (Fig. 2b). Additionally, both ultrasound and UV light facilitate the breakdown of O_3 molecules into micro-bubbles, improving its dissolution in water and producing reactive species such as electrons (e^-) and $^{\bullet}OH$. The high concentration of radicals generated through this combined approach significantly contributes to the mineralization of PE after 8 hours of treatment. Hu *et al.* 2023 coupled O_3 with H_2O_2 to increase the generation of $^{\bullet}OH$ for the removal of PE MPs.[36] The system containing 11.5 mg L^{-1} of O_3 and 20 mM H_2O_2 achieved approximately 33% mineralization of PE fragments (0.05 g L^{-1}, 40–48 μm in size). Li *et al.* developed a core–shell CeO_x@MnO_x catalyst to enhance the ozonation degradation of polystyrene NPs in water.[37] In this structure, the CeO_x core is enclosed by a MnO_x shell, allowing electron transfer from the core to the shell. This electron replenishment reduces the captured O_3 and promotes the generation of reactive oxygen species such as $^{\bullet}OH$, $^{\bullet}O_2^-$ and $^1O_2$ (Fig. 2c). Using 2.8 mg L^{-1} of O_3 and 5 mg L^{-1} of the catalyst, the system achieved ~97% degradation of spherical PS NPs ((2 mg L^{-1}, 80–300 nm in size). Similarly, Nieto-Sandoval *et al.* (2024) enhanced the mineralization of PS NPs to 70% by introducing Co^{2+} as a catalyst.[38] In the Co^{2+}/O_3 system, Co^{2+} facilitates ozone

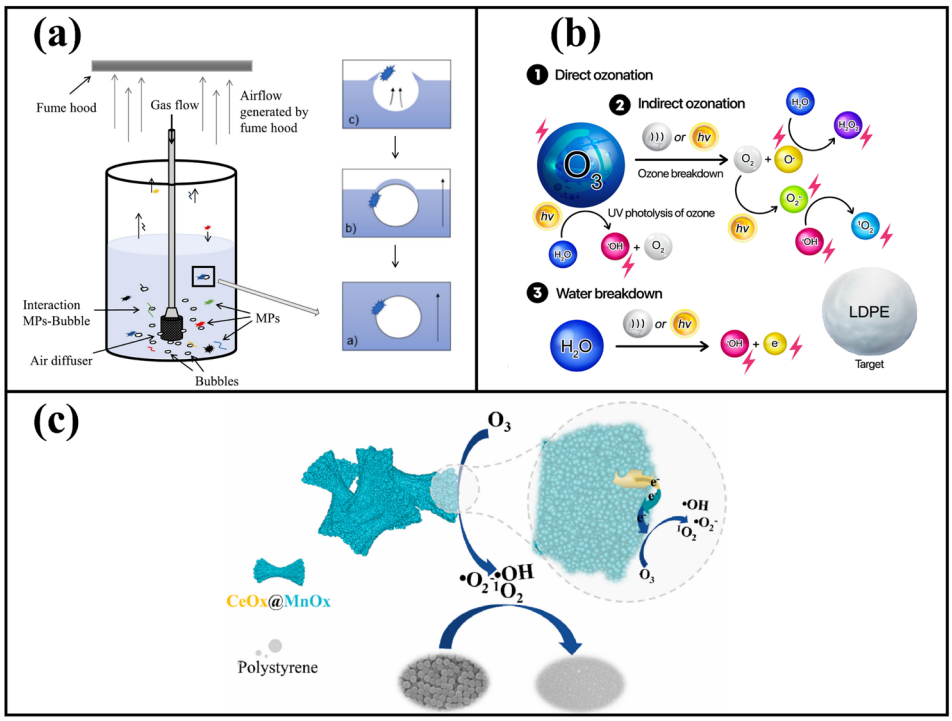

Fig. 2 Proposed mechanism for microplastic removal through physical entrainment induced by bubble bursting[28] (a) proposed dual pathways for the generation of reactive species: direct ozonation and water decomposition[35] (b), and schematic representation of the catalytic ozonation mechanism of polystyrene nanoplastics mediated by CeO_x@MnO_x[37] (c). Reprinted from ref. 28, Copyright (2023), and ref. 37, Copyright (2023) with permission from Elsevier. Adapted from ref. 35, Copyright (2025) with permission from Elsevier.

activation, forming $Co(OH)^{2+}$ and $^{\bullet}OH$ radicals. While $^{\bullet}OH$ contributes to the degradation of PS NPs, $Co(OH)^{2+}$ reacts with O_3 and OH^- to regenerate Co^{2+}, maintaing the catalytic cycle. These integrated approaches demonstrate that coupling ozonation with chemical additives, physical processes, or catalytic systems significantly enhances the generation of reactive species, thereby improving the degradation and mineralization efficiency of NMPs in aqueous environments. However, operational parameters were not optimized, particularly the ratio of O_3 to catalyst, and no post-treatment was applied to remove released metal ions after the treatment process. In addition, the system was evaluated only with readily degraded polystyrene, whereas more recalcitrant and widely encountered polymers, such as polyethylene and polypropylene, should also be examined to better assess treatment effectiveness.

Most studies on the ozonation of NMPs have been conducted at the laboratory scale, therefore, greater efforts and practical solutions are required to bridge the gap between experimental research and real-world applications. Pulido-Reyes *et al.* (2022) conducted pilot-scale experiments at a drinking water treatment plant to evaluate the applicability of lab-scale findings.[31] They examined how factors such as flow rate, filter bed depth, and pre-ozonation influenced nanoplastic retention. Results showed that ozone pretreatment had minimal effect on NP transport, as indicated by similar breakthrough curves for both treated and untreated particles.

Comparing ozonation with other AOPs is essential to properly assess its feasibility and effectiveness in practical treatment scenarios. According to Li *et al.*, ozonation and chlorination differ greatly in their ability to degrade nano-sized polystyrene in drinking water treatment.[34] At WHO-recommended disinfection levels, ozonation achieves 96% molecular weight reduction and 30% mineralization within 30 minutes, while chlorination shows minimal effect, with only 4% degradation and 3.0% mineralization. This highlights the resistance of polystyrene to chlorination and the superior efficiency of ozonation. The enhanced performance of ozonation is linked to its ability to introduce oxygen-containing groups, increasing the plastic's hydrophilicity and enabling further oxidation. A comparison between ozonation and wet oxidation highlights the greater effectiveness of wet oxidation for MP removal.[28] Under high-temperature conditions, wet oxidation achieved over 86% removal, while ozonation resulted in only about 45%. The limited performance of ozonation is primarily linked to the physical entrainment of MPs by the gas stream, rather than chemical breakdown. In contrast, wet oxidation, conducted in a closed system, promotes removal mainly through oxidative reactions with a significantly higher degradation rate. To better understand these mechanisms, Solís-Balbín *et al.* employed simulation and modeling to estimate the mass transfer of MPs from the liquid to gas phase. Their findings confirmed that in open ozonation systems, physical entrainment dominates, whereas in closed wet oxidation setups, chemical oxidation is the principal removal pathway. These results emphasize the value of incorporating modeling approaches in future studies to clarify removal mechanisms and guide process optimization.

Moreover, the cost of MP removal should be carefully determined in practical research and application, considering energy consumption for ozone generation, chemical usage, and potentially material synthesis. To estimate the energy efficiency of the process, Bolton's formula can be used to calculate the electrical energy required per unit of pollutant removed.[32] Accurate assessment of ozone consumption is essential, and it should be based on the actual transferred ozone dose rather than solely relying on the ozone concentration in the liquid phase or the inlet concentration in the gas stream.[38]

Ozonation-based AOPs show promise for NMP removal, but technological and safety limitations remain challenges for researchers. The stability of ozone in aqueous solution remains a concern, as it readily decomposes into species such as OH^-, HO_2^-, O_2^-, and $^{\bullet}O_2^-$.[29] This decomposition reduces the effective concentration of ozone available for the chemical degradation of NMPs. In addition, quantification methods for NMPs lack standardization and show significant variation. Optical microscopy is subjective, only quantifies NMPs retained by the selected filter membrane, is time-consuming, and prone to errors. In NMP treatment studies, optical microscopy mainly helps assess the extent of degradation but cannot determine complete removal or mineralization.[28] Similarly, gel permeation chromatography with certain limit of detection, can only evaluate the degradation effectiveness of ozonation rather than total removal.[37] Total organic carbon analyzer is helpful in analyzing the mineralization of NMPs.[35,38] However, according to Hu *et al.*, since the breakdown of long-chain NMPs can lead to an increase in soluble organic by-products, and these compounds only decline as they are further mineralized to CO_2, changes in TOC levels in the solution do not reliably reflect the extent of mineralization.[36] To accurately assess mineralization, the authors recommended using a closed system connected to a NaOH solution captures the CO_2 generated during the ozonation of MPs. In this setup, the amount of inorganic carbon absorbed served as an indicator of CO_2 production and, consequently, the degree of mineralization. Due to the absence of reliable analytical methods for detecting nanoplastics in complex matrices, Pulido-Reyes *et al.* employed a metal-labeling approach.[31] NPs were tagged with palladium (Pd), enabling their quantification using Pd as a tracer. The concentration of Pd was then determined through inductively coupled plasma mass spectrometry. Few studies have addressed the potential environmental impacts of NMP-containing water following treatment. For example, Pattanateeradetch *et al.* investigated this aspect by conducting germination tests on three types of vegetable seeds to assess the toxicity of treated water.[35] Their findings suggested that delayed seed germination may result from the transformation of MPs into NPs, which can accumulate in the plant vascular system and disrupt water and nutrient uptake.

3. Photocatalytic treatment of NMPs

Photocatalysis has long been recognized as an effective approach within AOPs for mitigating water pollution. It involves activating a solid photocatalyst with light energy to generate reactive oxygen species, which can break down persistent contaminants into less harmful compounds. This process relies on semiconductor materials that, upon absorbing photons with sufficient energy, produce electron–hole pairs that drive redox reactions in aqueous environments.[40] A major advantage of photocatalysis is its ability to harness solar energy, making it a sustainable option for aquatic pollution control.

While widely studied for environmental remediation, its application to NMPs remains limited and presents several challenges. Key issues include a limited understanding of the degradation pathways for various NMP types, reduced photocatalytic performance under visible light conditions, and practical obstacles in catalyst recovery and reuse during treatment processes in real aquatic environments. For example, in one of the initial studies in this direction, Jeyaraj and colleagues synthesized TiO_2 nanoparticles, one of the most widely used catalysts globally, to treat polypropylene MPs under solar light irradiation.[41] Although various techniques such as FT-IR, UV-Vis DRS, ^{1}H-NMR, and FE-SEM have been employed to investigate the degradation mechanisms of MPs, several aspects remain unclear and continue to raise questions. In addition to the prolonged processing time of 100 hours, the post-treatment procedure for removing TiO_2 from the MP surface was not clearly described. Moreover, assessing MP removal efficiency based solely on the weight loss of filtered MPs is unreliable, as partially degraded MPs may fragment into smaller particles that pass through the filter and remain suspended in the solution with TiO_2, potentially leading to secondary pollution. Furthermore, certain technical issues remain unaddressed, such as the inability of photogenerated holes in TiO_2 to effectively oxidize water and produce hydroxyl radicals, which are critical for MP degradation.

The rapid recombination of electron–hole pairs in many semiconductor photocatalysts remains a major limitation. To address this, the construction of semiconductor composites with heterojunctions has been explored, as it enhances surface properties, promotes efficient charge separation, and improves light harvesting, thereby increasing overall photocatalytic performance. In a representative study, Zhang *et al.* synthesized $BiOCl/Cs_3Bi_2Br_9$ composites for the photocatalytic degradation of polystyrene MPs.[42] Using 0.1 g L^{-1} of the optimized composite under xenon lamp irradiation at neutral pH, approximately 42% of the microplastics were degraded after 50 hours of treatment (Table 3). Reactive oxygen species were reported to initiate polystyrene degradation by forming radicals that react with oxygen to produce unstable intermediates. These undergo hydrogen abstraction, bond cleavage, and molecular rearrangement, leading to smaller compounds that ultimately oxidize into CO_2 and H_2O. The difference in work functions between the semiconductor components creates an internal electric field at their interface. This field facilitates effective charge carrier separation *via* the S-scheme heterojunction mechanism, thereby enhancing the overall system performance (Fig. 3a). Similarly, Cao *et al.* developed a hydroxyl-rich BiOCl/TiO_2 composite for treating polyethylene MPs.[43] When 1.5 g L^{-1} of the optimized material was exposed to xenon lamp irradiation for 20 hours, it resulted in a 63% weight loss of the MPs.

Table 3 Overview of the recent studies using photocatalysis-based processes for MNP treatment

Photocatalyst	NMPs (conc., type, shape, size)	Operational conditions	Removal efficiency and degradation rate	References
TiO_2 nanoparticle	Polypropylene MPs (4 g L^{-1}, sphere, 12 μm)	Solar irradiation Catalyst dose: 4 g L^{-1} Time: 50 h pH 3 Temperature: 37–40 °C	Weight loss: ~51%	41
ZnO nanoparticle	Polypropylene MPs (1 g L^{-1}, sphere, ~150 μm)	Natural sunlight Catalyst dose: 1 g L^{-1} Time: 24 h pH 7	Weight loss: 50%	44
$Cs_3Bi_2Br_9$/BiOCl	Polystyrene MPs (1 mg L^{-1}, sphere, ~150 μm)	Xenon lamp (300W) Catalyst dose: 0.1 g L^{-1} Time: 50 h pH 7	Weight loss: 42%	42
OH-rich BiOCl/TiO_2	Polyethylene MPs (2.5 g L^{-1})	Xenon lamp (300W) Catalyst dose: 1.5 g L^{-1} Time: 20 h	Weight loss: 63%	43
Fe-doped BiO_{2-x}/BiOI	Polyethylene terephthalate MPs (0.5 g L^{-1})	Xenon lamp (500 W) Catalyst dose: 0.5 g L^{-1} Time: 1 h	No removal info	45
O/S doped C_3N_4	Polyethylene MPs (~300 μm)	Xenon lamp (68.0 mW cm^{-2}) Catalyst dose: 0.04 g L^{-1} Time: 8 days pH 3	Weight loss: 44%	46
Co^{2+}-substituted $ZnFe_2O_4$/ZnO	Polypropylene MPs	Halogen lamp (1000 W m^{-2}) Catalyst dose: 3 g L^{-1} Time: 20 h	Weight loss: 18% Degradation: 98% $k = 0.035 \pm 0.001$ min^{-1}	47
CoNiFe($V_{Zn\text{-}Al}$)-LDHs + PMS (5 mM L^{-1})	Polyethylene MPs (5 g L^{-1})	Xenon lamp (300 W) Catalyst dose: no info PMS: 5 mM L^{-1} Time: 10 h pH 7 Temperature: 95 °C Flow rate: 40 mL min^{-1}	Weight loss: 100% Mineralization: 33%	48
TiO_2/chitin sponge	Polystyrene MPs (0.02 g L^{-1}, 1 μm)	UV lamp (60 W) Time: 6 h pH 3 Temperature: 35 °C	UV-VIS absorbance: 58% $k = 0.159$ h^{-1}	49
C,N–TiO_2/CNF aerogel	Polyethylene MPs (1 g L^{-1})	UV lamp (254 nm) Catalyst dose: 7 mg L^{-1} pH 3	Weight loss: 18.5%	50
ZnO NRs/glass fiber	Polypropylene MPs (10^4 particles L^{-1}, sphere, 155 μm)	Tungsten-halogen lamp (120 W) Catalyst dose: 17 g L^{-1} Time: 19 days Continuous flow: 0.3 L min^{-1}	No removal info	51
Ag/TiO_2/ceramic membrane	Polyester MPs (fibers, <1000 μm)	UVC lamp Time: 48 h	Weight loss: 23.2%	48
C_3N_4/$Bi_{12}O_{17}Cl_2$/PAN membrane	Polylactic acid MPs (2 g L^{-1})	Xenon lamp (300W) Time: 12 h	No removal info	52
TiO_2/membrane + $Na_2S_2O_8$	Polyester NMPs (0.1 g L^{-1})	Hg lamp Catalyst dose: 0.5 g L^{-1} $Na_2S_2O_8$: 0.5 g L^{-1} Time: 48 h pH 10 Temperature: 30 °C	Weight loss: 13.5%	53
MXene/$Zn_xCd_{1-x}S$	Polyethylene terephthalate (no other infos.)	Xenon lamp (300 W) Catalyst dose: 0.002 g L^{-1}	No removal info	54
WO_3/g-C_3N_4	Polyethylene terephthalate MPs (0.5 g L^{-1})	Xenon lamp (300 W) Catalyst dose: 2 g L^{-1}	No removal info	55
$CuInSe_2$/CdS	Polyethylene terephthalate MPs (25 g L^{-1})	Xenon lamp (300 W) Catalyst dose: 0.5 g L^{-1} Time: 3 h pH: highly basic	No removal info	56

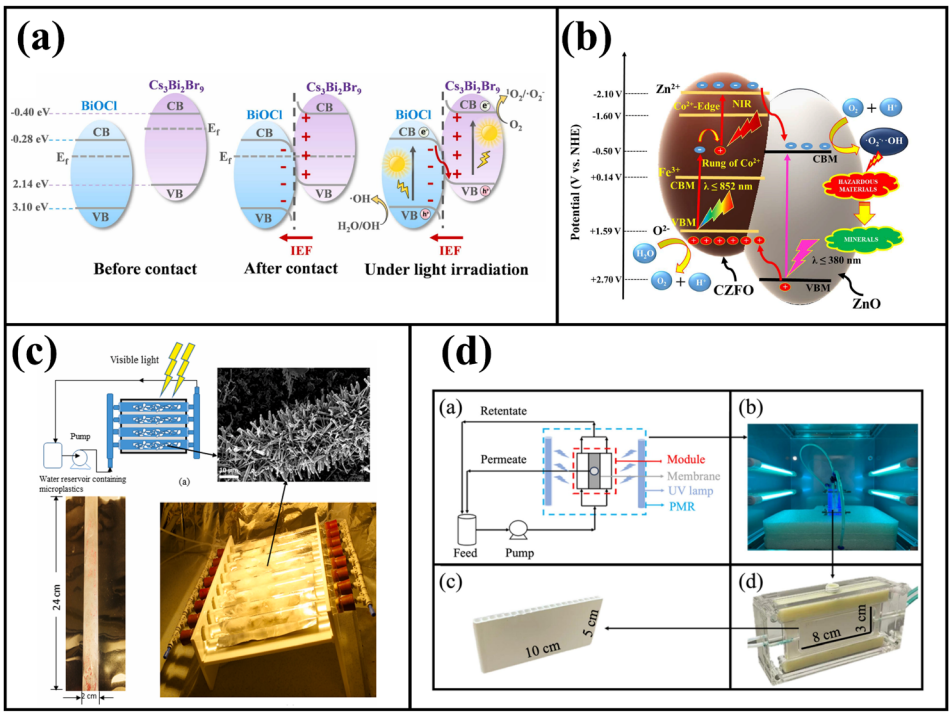

Fig. 3 S-scheme photocatalytic mechanism of $Cs_3Bi_2Br_9$/BiOCl composite for polystyrene MP degradation[42] (a), photocatalytic mechanism of Co^{2+}-substituted $ZnFe_2O_4$/ZnO, highlighting Co^{2+} and Zn^{2+} levels enabling laddered-like charge transfer[47] (b), photocatalytic reactor with ZnO-nanorod-coated glass fibers for polypropylene MP treatment[51] (c), and diagram of Ag/TiO_2/ceramic photocatalytic membrane module[48] (d). Adapted from ref. 42, Copyright (2025) and ref. 47, Copyright (2024) with permission from Elsevier. Reproduced from ref. 51 under the terms of the Creative Commons CC BY license. Reprinted from ref. 48, Copyright (2025) with permission from Elsevier.

The integration of BiOCl with TiO_2 generates an internal electric field directed from BiOCl to TiO_2, which facilitates charge carrier separation through a type-II heterojunction. However, this mechanism raises a question because, despite the spontaneous migration of electrons from TiO_2 to BiOCl until Fermi level alignment, the energy positions of the conduction and valence bands remain fixed. Consequently, electron transfer from the conduction band of TiO_2 to BiOCl occurs in the opposite direction to the established electric field. Microwave pretreatment was reported to induce structural changes and reduce polymer chain entanglement, which enhance the degradation rate of MPs. However, the process involves high energy consumption, requiring continuous heating at 100 °C for 10 hours using 600 W power. This significant energy demand limits the practical applicability of the method.

In addition to composite fabrication, metal doping is a commonly employed approach to enhance the photocatalytic efficiency of semiconductor materials. For example, Liu *et al.* investigated the effect of iron doping on a BiO_{2-x}/BiOI composite for the degradation of polyethylene terephthalate microplastics.[45] The introduction of Fe into BiO_{2-x} was found to increase the Fermi level difference between BiO_{2-x} and BiOI, thereby strengthening the driving force for directional electron transfer and improving charge separation, which contributes to enhanced photocatalytic performance. Although the rise in TOC values after treatment indicates the breakdown of MPs, no additional experiments were carried out to assess the extent of mineralization or to separate the catalyst from the resulting intermediate compounds. Another limitation is the requirement of alkaline pretreatment for PET to induce hydrolysis and weaken the polymer backbone prior to further treatment. In another study on polyethylene MPs degradation,[46] Luo *et al.* enhanced the photocatalytic performance of g-C_3N_4 by co-doping it with oxygen and sulfur. This modification significantly narrowed the bandgap of the material, promoting more efficient excitation and transfer of photoinduced electrons. As a result, the O/S-doped g-C_3N_4 achieved four times greater degradation efficiency, causing a 44% weight loss of MPs after 8 days of simulated solar irradiation, compared to undoped g-C_3N_4. Further work is required to shorten the prolonged reaction time. Moreover, while the MP were collected, centrifuged, and lyophilized, the method used to separate the photocatalyst from the MP particles was not clearly reported. Lopis *et al.* investigated the photocatalytic degradation of polypropylene MPs derived from face masks by incorporating Co^{2+} into a core–shell $ZnFe_2O_4$/ZnO composite.[47] The introduction of Co^{2+} facilitated the formation of a ladder-type I heterojunction by supplying ground-state electrons to the conduction band, which broadened the light absorption of the composite across a wider wavelength range (Fig. 3b). The optimized composite demonstrated a 6-fold increase in the degradation rate constant for methyl orange compared to the undoped photocatalyst but achieved only 18% degradation of polypropylene MPs after 20 hours of solar irradiation.

An effective strategy in AOPs for degrading NMPs in water is using of photocatalyst to activate oxidants like hydrogen peroxide and persulfate species under light irradiation, generating highly reactive oxygen species that drive NMPs degradation. In a typical study, Wu *et al.* developed an advanced high-entropy layered double hydroxide (LDH)-based photocatalyst by introducing and etching high-valence metals such as Fe, Co, and Ni into the Zn/Al sites of the LDH structure.[57] This modification enhanced peroxymonosulfate (PMS)-assisted photocatalytic degradation of MPs. The dynamic exchange of Zn and Al reduced the d-orbital occupancy of the metal centers, improving solar light absorption and charge separation. As a result, the catalyst effectively activated PMS to generate reactive species including $^{\bullet}OH$, $^{\bullet}SO_4^-$, and $^1O_2$, enabling the conversion of one-third of polyethylene MPs (5 g L^{-1}) into CO_2 within 10 hours under visible light.

Recovering the photocatalyst after water treatment is essential for both practical application and environmental sustainability. Meng *et al.* incorporated TiO_2 into a chitin-based matrix to enhance the degradation of polystyrene MPs.[49] The chitin sponge's porous structure and functional groups enhance MP capture, promoting better contact with TiO_2 and boosting photocatalytic activity. The TiO_2/chitin composite achieved 59% degradation within 6 hours under UV light. Additionally, the composite could be easily recovered after treatment, highlighting its practical applicability for reuse. One drawback of the system is the prolonged 24 hour dark period required to reach adsorption–desorption equilibrium with MPs, which lengthens the overall treatment time. Similarly, Motenegro *et al.* incorporated a C,N-doped TiO_2 photocatalyst into a cellulose-based aerogel for the treatment of polyethylene MPs in water.[50] Photocatalysis played a minor role in the removal process, contributing to a 19% weight loss. While the aerogel functioned as a photocatalyst support, it also facilitated physical capture of MPs through collisions among spherical particles. However, maintaining an optimal pH of 3 introduces practical, economic, and environmental limitations, hindering scalability. Organic carriers, particularly those derived from bio-based sources, are lightweight, low-cost, and easy to fabricate, but they tend to degrade under photocatalytic conditions. To overcome these limitations, Uheida *et al.* (2021) investigated the use of glass fiber substrates for immobilizing ZnO nanorods in the photocatalytic degradation of polypropylene microplastics under continuous flow conditions.[51] The glass fibers not only provided stable support for ZnO but also helped trap microplastics, enhancing their interaction with the photocatalyst (Fig. 3c). After two weeks of visible light exposure, the average particle volume of microplastics was reduced by 65%. However, using optical microscopy to monitor particle size distribution during the process offered only a partial assessment of the actual removal efficiency.

Some studies have integrated photocatalysis with additional water treatment techniques to enhance MP removal through synergistic effects. In one such work, Biao *et al.* fabricated a photocatalytic membrane by loading Ag/TiO_2 onto a ceramic substrate, enabling the simultaneous application of photocatalysis and filtration for the treatment of polyester MPs in laundry effluent[48] (Fig. 3d). After 48 hours of UVC irradiation, the Ag/TiO_2 photocatalytic membrane achieved 23% degradation of MPs and significantly improved the membrane's antifouling performance. However, the practice of recirculating permeates back to the feed to assess microplastic degradation is not representative of real-world water treatment operations. The absence of mechanistic analysis limits understanding of the photocatalytic process. Additionally, the comparison of degradation rates and rejection performance at varying initial MP concentrations was not appropriately conducted. The study also overlooked that photocatalysis could generate smaller MPs, potentially reducing filtration performance. In a related approach, Wu *et al.* fabricated a photocatalytic membrane by electrospinning a $C_3N_4/Bi_{12}O_{17}Cl_2$ photocatalyst onto a polyacrylonitrile substrate for continuous-flow treatment of effluents containing pharmaceuticals and polylactic acid MPs.[52] As in the previous study, the permeate was recirculated to the feed, however, the membrane functioned solely as a support for the photocatalyst in this case. Consequently, antifouling performance was not evaluated, and removal efficiency was attributed entirely to photocatalytic activity, making the recirculation approach reasonable. However, the efficiency of MP removal was not clearly established, as the authors reported only the intermediates formed during photocatalysis rather than directly quantifying the remaining MPs. Poerio *et al.* employed a two-step process combining filtration and photocatalysis for the treatment of polyester MPs.[53] Initially, a nanomembrane was used to concentrate the MP suspension, providing a more suitable feed for subsequent photocatalytic treatment. In the second stage, TiO_2 was utilized to activate sodium persulfate, a strong oxidant, resulting in a 14% weight loss of MPs (100 mg L^{-1}) after 48 hours of irradiation with a mercury lamp. The integration of membrane separation with photocatalysis offers a promising approach for efficiently removing NMPs from contaminated water. H_2O_2 was also tested as a reference oxidant; however, the study did not provide a detailed comparison or clear conclusion regarding its relative oxidation performance.

In summary, research on photocatalysis for the treatment of NMPs in water has only gained attention in recent years but has already achieved encouraging initial results. Studies have focused on modifying the electronic structure by metal doping and forming composites from two or three semiconductor materials to improve photocatalytic activity in NMP degradation. Catalyst recovery after treatment has been improved by immobilizing the material on floating supports,[50] fibers,[49] or membranes,[53] or by developing magnetic photocatalysts for easy separation.[47] Photocatalysts have also been employed to activate oxidizing agents, increasing the production of strong reactive radicals for NMP breakdown. Some works have integrated computational chemistry methods, such as density functional theory (DFT), to analyze the electronic structure and catalytic mechanisms of the materials.[42,45,46,52] The transformation pathways of NMPs and the formation of by-products during degradation have been investigated in detail using advanced analytical techniques, including HPLC, Py-GC/MS, GC-TOF-MS, ^1H NMR, and XPS.[41,42,44,46,48,49,51,52,54,55] The

potential toxicity of treated water, which could pose risks to both the environment and human health, has been assessed through experimental tests, such as evaluating effects on algal growth[42] and *E.coli*,[57] as well by examining the toxicity of degradation by-products using online databases on hazardous substances.[51] A few studies have explored the multifunctional use of photocatalysts, demonstrating their ability to simultaneously degrade NMPs and produce hydrogen,[54–56] as well as to remove other contaminants such as antibiotics, dyes, and harmful bacteria.[42,47,52] In addition, energy consumption has been evaluated to optimize operational parameters and improve the practicality of these processes.[48]

Despite promising results, the application of photocatalysis for NMP degradation still faces numerous challenges. One major limitation is the difficulty in separating the catalyst from microplastics after treatment, which can lead to inaccurate assessments of degradation efficiency. Most studies have evaluated removal efficiency based on the mass of NMPs recovered using membrane filtration, a method that strongly depends on the membrane pore size and often overlooks particles small enough to pass through. Many catalytic systems only operate effectively under harsh conditions, such as highly acidic or alkaline pH,[41,50,53,56] elevated temperatures,[48] or prolonged reaction times,[51] which limits their feasibility for real-world applications compared to their initial laboratory-scale demonstrations. Research has also given little attention to photocatalyst recovery and reuse, testing real wastewater samples, or scaling up the process. Moreover, most studies report incomplete MP degradation, producing numerous by-products and, in some cases, catalyst leaching. This highlights the need to evaluate the environmental impact and toxicity of effluents containing degradation intermediates, as well as to develop strategies for post-treatment management of photocatalyst-treated water.

4. Fenton-based processes for the treatment of NMPs

The Fenton process is a popular advanced oxidation technique in which ferrous ions (Fe^{2+}) activate hydrogen peroxide (H_2O_2) to produce hydroxyl radicals ($^{\cdot}OH$), highly reactive species capable of decomposing resistant pollutants. In this mechanism, Fe^{2+} is oxidized to Fe^{3+}, while subsequent reactions with H_2O_2 regenerate Fe^{2+}, maintaining a continuous radical-producing cycle (eqn (7) and (8)).

$$Fe^{2+} + H_2O_2 \rightarrow Fe^{3+} + {}^{\cdot}OH + OH^- \quad (7)$$

$$Fe^{3+} + H_2O_2 \rightarrow Fe^{2+} + {}^{\cdot}HO_2 + H^+ \quad (8)$$

Initially limited to the classical homogeneous system requiring acidic pH, it has since advanced into variants such as Fenton-like reactions with alternative metals, photo-Fenton using light for Fe^{2+} regeneration, electro-Fenton with *in situ* H_2O_2 generation, and heterogeneous catalysts (*e.g.*, iron oxides, nanomaterials, MOFs) that reduce sludge and improve reusability. In recent years, different Fenton-based approaches have been explored for the degradation of NMPs (Table 4). In 2022, Ortiz *et al.* employed a conventional Fenton system to investigate the degradation of NMPs with different particle sizes.[58] Using Fe^{3+} at 10 mg L^{-1} and H_2O_2 at 1 g L^{-1}, the process induced significant surface oxidation of polystyrene microplastics but achieved only limited degradation, with about 10% weight loss after 7.5 hours under harsh conditions (pH 3, 80 °C) (Fig. 4a). Degradation efficiency increased as MP particle size decreased, with higher weight loss and lower H_2O_2 consumption observed for smaller particles. This trend indicates that oxidation primarily occurs at the particle surface, where $^{\cdot}OH$ attack the exposed polymer. In contrast, the same treatment was more effective for nanoplastics, achieving nearly 70% reduction in TOC for polystyrene NPs (0.02 g L^{-1}). While the study confirmed that the intermediates generated were biodegradable, it did not address the issue of iron removal after treatment. Similarly, Liu *et al.* evaluated the degradation of polystyrene and Nylon 6 microplastics using both Fe^{2+}/H_2O_2 and Fe^{2+}/PMS systems.[59] The Fe^{2+}-activated PMS process exhibited superior performance compared to the traditional Fenton reaction, achieving 22–26% weight loss *versus* 14–17%, and was also able to mineralize the resulting aromatic intermediates owing to the higher oxidative potential of sulfate radicals.

Di Luca *et al.* reported that photo-assisted Fenton treatment shows far greater efficiency than the classical process in removing nanoplastics. In their study, a system containing Fe^{3+} (1 mg L^{-1}) and H_2O_2 (130 mg L^{-1}), irradiated with a 150 W Hg lamp, was able to completely mineralize 0.02 g L^{-1} of polystyrene NPs within 40 minutes.[60] The enhanced performance was attributed not only to the standard Fenton reactions but also to additional radical generation through photolysis of H_2O_2 and the light-induced activation of Fe^{3+} species. However, it is inappropriate to present the classical Fenton process under dark conditions as yielding no TOC removal, since this overlooks the fact that the standard Fenton reaction itself can generate significant hydroxyl radicals capable of driving oxidation. In their follow-up study,[61] this group succesfully identified suitable models for polystyrene NP degradation by photo-Fenton process. Oxidation proceeds progressively from the particle surface toward the core until complete disappearance. Among the models tested, the Shrinking Core Model offered the best description of the conversion behavior, suggesting that the reaction rate is governed by surface chemical processes rather than mass-transfer limitations, which are negligible at the nanoscale. In addition, the Prout–Tompkins model was able to capture the overall conversion trend of polystyrene NPs.

Fe-based catalysts improve on classical and photo-Fenton systems by working over a broader pH range, producing little sludge, and allowing easy recovery and reuse, which enhances both efficiency and sustainability. Wu *et al.* synthesized and applied Fe-based piezo-catalyst $Bi_{12}(Bi_{0.5}Fe_{0.5})O_{19.5}$ to activate H_2O_2 for the treatment of polyethylene terephthalate MPs.[62] $Bi_{12}(Bi_{0.5}Fe_{0.5})O_{19.5}$ shows strong piezoelectricity, where ultrasonication disturbs interfacial polarization and induces band-to-band transitions, producing electron–hole pairs. These charges, together with Fe-mediated H_2O_2 activation, drive the

Table 4 Overview of the recent studies using Fenton-based processes for MNP treatment

Fenton system	NMPs (conc., type, shape, size)	Operational conditions	Removal efficiency and degradation rate	References
Fe^{3+} + H_2O_2	Polystyrene MPs (1.3 g L^{-1}, 150–250 μm) Polystyrene NPs (0.02 g L^{-1}, 140 nm)	Fe^{3+} dose: 10 mgL^{-1} H_2O_2 dose: 1 g L^{-1} for MPs 130 mg L^{-1} for NPs Time: 7.5 h pH 3 Temperature: 80 °C	Weight loss: 10% Mineralization: 70% (TOC)	58
Fe^{3+} + H_2O_2	Polystyrene MPs (0.5 g L^{-1}) Nylon 6 MPs (0.5 g L^{-1}) Weight loss: 14%	Fe^{2+} dose: 3 mM H_2O_2 dose: 0.5% pH 3	Weight loss: 17%	59
Fe^{3+} + H_2O_2 + light	Polystyrene NPs (0.02 g L^{-1}, nanosphere, 140 nm)	Hg lamp (150 W) Fe^{3+} dose: 1 mgL^{-1} H_2O_2 dose: 130 mg L^{-1} Time: 40 min pH 3 Temperature: 25 °C	Mineralization: 100% (TOC) $k = 0.09$ min^{-1}	60
Fe^{3+} + H_2O_2 + light	Polystyrene NPs (0.1 g L^{-1}, nanosphere, 140 nm)	Hg lamp (150 W) Fe^{3+} dose: 1 mgL^{-1} H_2O_2 dose: 1000 mg L^{-1} Time: 80 min pH 3 Temperature: 25 °C	Mineralization: 100% (TOC)	61
$Bi_{12}(Bi_{0.5}Fe_{0.5})O_{19.5}$ catalyst + H_2O_2	Polyethylene terephthalate MPs (10 g L^{-1})	Ultrasonic cleaner (120 W, 40 kHz) Catalyst dose: 0.5 g L^{-1} H_2O_2 dose: 240 mM Time: 72 h	Weight loss: 29%	62
FeOCl/CNT catalyst + H_2O_2	Polyvinyl chloride NPs (0.02 g L^{-1}, 20 nm)	Catalyst dose: 0.1 g L^{-1} H_2O_2 dose: 0.34 g L^{-1}	27.3% (chloride release)	63
MIL-101(Fe)/BiOI photocatalyst + H_2O_2	Polyethylene MPs (1 g L^{-1}, microsphere, 230 μm)	Xenon lamp (500 W) Catalyst dose: 1 g L^{-1} H_2O_2 dose: 130 mg L^{-1} Time: 6 h	No removal info	64
$Fe_{1-x}S/FeMoO_4/MoS_2$ photocatalyst	Polystyrene MPs (5 g L^{-1})	Ultrasonic cleaner (120 W, 40 kHz) LED lamp (24 W) Catalyst dose: 2.5 g L^{-1} Time: 1 h	Weight loss: 58.5%	65
O_2/N_2 + Fe + *S. putrefaciens* bacteria	Polystyrene MPs (5 g L^{-1}, sheet, 5 mm)	Fe^{3+} dose: 10 mM Time: 14 days pH 7 Temperature: 25 °C Aerobic condition: air sparging Anaerobic condition: N_2 sparging	Weight loss: 6.1%	66

generation of reactive oxygen species. Treatment of 0.1 g L^{-1} microplastics in an ultrasonic cleaner (120 W, 40 kHz) with 0.5 g L^{-1} catalyst and 240 mM H_2O_2 for 72 h resulted in a 29% weight loss. Both computational predictions and mung bean germination tests showed that the degradation intermediates are less toxic than the parent MPs, with some essentially non-toxic, and do not inhibit plant growth. Further studies should focus on reducing the energy demand, as 72 hours of high-power sonication is not a practical approach. In another notable study, Sun *et al.* addressed the limitations of pollutant transport and the short lifetime of hydroxyl radicals by designing a catalyst system that integrates FeOCl within carbon nanotubes (CNTs).[63] The confined space inside the CNTs reduced the distance between FeOCl active sites and small pollutants, enhancing catalytic efficiency. Meanwhile, electron penetration on the outer surface of the CNTs facilitated rapid Fenton reactions, enabling the degradation of larger pollutants like PVC microplastics (Fig. 4b). Nevertheless, the degradation of PVC MPs was not comprehensively analyzed, as the study only reported chloride ion release of 27.3%. Interestingly, the presence of H_2O_2 significantly suppressed iron leaching, reducing dissolved Fe concentrations to 0.94 μg L^{-1} compared with 53 μg L^{-1} in the absence of H_2O_2, highlighting its role in stabilizing the catalyst and limiting secondary contamination.

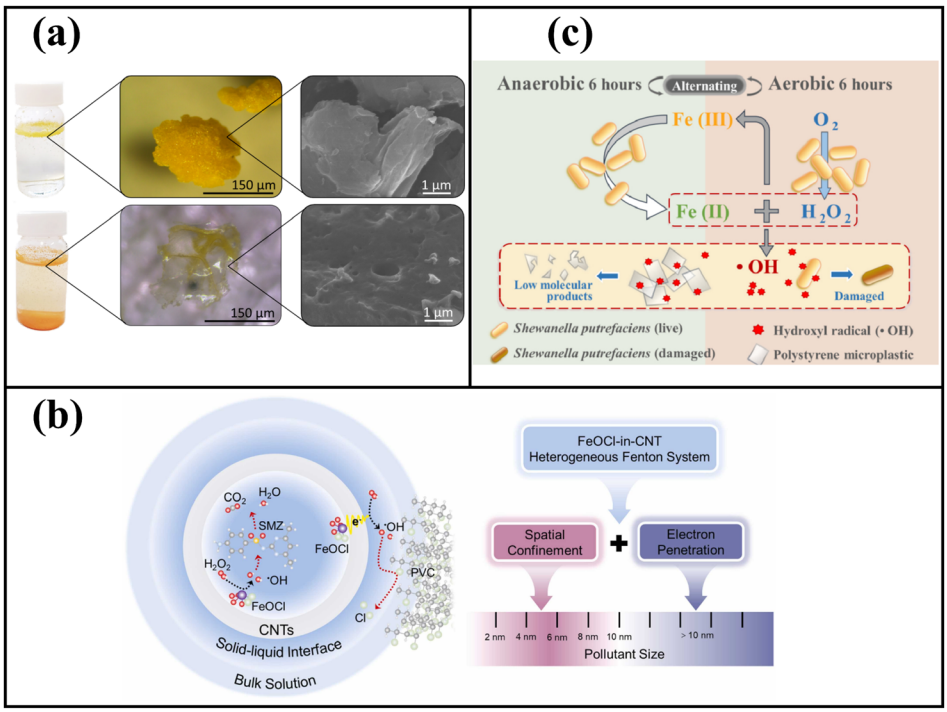

Fig. 4 Microscopic and SEM images of polystyrene microplastics before and after Fenton-based treatment[58] (a), schematic illustration of the catalytic activity of the FeOCl/CNT system in PVC MP degradation[63] (b), and schematic representation of the bio-Fenton process using *S. putrefaciens* for polystyrene MP degradation[66] (c). Reprinted from ref. 58, Copyright (2022), ref. 63, Copyright (2025), and ref. 66, Copyright (2022) with permission from Elsevier.

In another approach, the heterogeneous photo-Fenton system, employing iron-based photocatalysts rather than soluble iron salts, was explored for the treatment of NMPs. For instance, Gu *et al.* developed a MIL-101/BiOI heterojunction composite for activating H_2O_2 in the degradation of polyethylene MPs.[64] In this design, BiOI acted as a semiconductor partner, while the MIL-101 contributed both Fe^{3+}/Fe^{2+} redox activity and photosensitive Fe–O clusters, thus, enhancing H_2O_2 activation. $^{\bullet}OH$ initiate PE degradation by forming carbon-centered radicals, which react with O_2 to generate peroxy species and unstable peroxides. These intermediates undergo decomposition, chain scission and Norrish-type reactions, producing oxygenated fragments with lower molecular weight. Continued oxidation ultimately mineralizes the intermediates to CO_2 and H_2O. Despite these innovations, the study left several aspects insufficiently addressed. Although the catalyst was presented as promising with potential for industrial application, the reported findings were limited to surface oxidation of the MPs, with no data of bulk degradation. Moreover, the photocatalytic mechanism was not convincingly elucidated when experimental validation of band energy levels was lacking. Lu *et al.* developed a novel piezo-photocatalyst, $Fe_{1-x}S/FeMoO_4/MoS_2$, capable of initiating self-Fenton reactions to degrade polystyrene microplastics without the external addition of H_2O_2.[65] At a dosage of 2.5 g L^{-1}, the photocatalyst showed high efficiency, leading to a high 58.5% weight loss of polystyrene MPs after 1 h of treatment under simultaneous 24 W LED irradiation and 40 kHz ultrasonication. The authors deserve credit for employing multiple techniques to investigate the piezoelectric effect, band potentials, H_2O_2 and radical generation, as well as the degradation pathways of MPs. Although the Fermi levels of the individual materials were reported, their alignment after interfacial contact was not clarified, leading to a misleading description of band bending and charge transfer. For instance, because MoS_2 has a lower work function than $Fe_{1-x}S$, electrons should migrate from MoS_2 to $Fe_{1-x}S$ upon contact to reach Fermi level equilibrium, resulting in upward band bending in MoS_2. Under this configuration, the internal electric field, together with the more negative CB and VB positions of $Fe_{1-x}S$ compared to MoS_2, would drive holes from the VB of MoS_2 to the VB of $Fe_{1-x}S$ and electrons from the CB of $Fe_{1-x}S$ to the CB of MoS_2. This expected charge transfer pathway contrasts with the mechanism proposed by the authors.

Unlike the chemical strategies mentioned above, Yang *et al.* explored a bio-Fenton approach in which bacteria were employed to initiate the reaction for polystyrene MP degradation.[66] During aerobic respiration, *Shewanella putrefaciens* generate H_2O_2 through the incomplete reduction of O_2, while under anaerobic conditions it reduces Fe^{3+} to Fe^{2+}, enabling the Fenton process (Fig. 4c). More hydrophilic surfaces were more readily colonized by microorganisms, promoting further degradation. Chain scission generates terminal radicals that react with O_2 to form peroxy radicals, leading to the formation of oxygenated groups (–OH, –C=O, –COOH). Continued oxidation progressively breaks the polymer into low-molecular-

weight products. However, this approach presents several challenges: the cultivation of bacteria and the need to alternate between aerobic and anaerobic environments make the process costly, and despite a prolonged reaction time of 14 days, only 6% weight loss of polystyrene MPs was achieved. In addition, the radicals produced also damaged the bacteria themselves, with cell viability dropping to 66% after 48 hours.

To sum up, the limitations associated with post-treatment of iron ions and the acidic operating conditions in conventional Fenton and photo-Fenton processes have been mitigated by heterogeneous Fenton systems, with piezo-photocatalysts under light and ultrasound showing notable performance. Recent studies have also employed advanced analytical methods, such as pyrolysis-GC/MS, to investigate the structural transformation of degradation intermediates, thereby providing valuable insights into their potential environmental risks. However, the evaluation methods across studies remain inconsistent. Some works focus only on detecting surface oxidation of NMPs through the introduction of oxygen-containing functional groups, while others assess degradation efficiency based on weight loss. The latter approach is strongly dependent on membrane filtration of residual particles, which complicates comparisons due to variations in the size and molecular weight of the initial plastics. In addition, discrepancies in understanding catalytic pathways and H_2O_2 activation are often linked to limited access to advanced instrumentation capable of analyzing the electronic properties of catalysts. Polystyrene NMPs are commonly studied due to their prevalence and persistence, while computational methods are increasingly applied to probe catalyst–plastic interactions and predict intermediate toxicity. Economic feasibility is also a concern, as approaches like bacteria-assisted Fenton or microwave treatment can be highly energy- and cost-intensive.

5. Electrochemical processes for the treatment of NMPs

Electrochemical (EC) processes represent advanced and sustainable AOPs for water treatment, utilizing applied electrical energy to initiate redox reactions at electrode interfaces. These reactions enable the direct degradation of contaminants or the *in situ* generation of reactive species.

Recent studies on electrochemical treatment of NMPs emphasize cathodic processes, where pollutants can be degraded either through direct electron transfer or *via* indirect pathways involving reactive oxygen species. In the indirect route, O_2 undergoes a two-electron reduction to form H_2O_2 (eqn (9)), which can be further electroreduced to $^{\bullet}OH$ (eqn (10)), thereby driving pollutant degradation.[67] For these reactions to proceed efficiently, the cathode material must be carefully designed to suppress the competing hydrogen evolution reaction (eqn (11)):[67]

$$O_2 + 2H^+ + 2e^- \rightarrow H_2O_2\ (E^0 = +0.695\ \text{V}\ \textit{vs.}\ \text{NHE}) \quad (9)$$

$$H_2O_2 + e^- \rightarrow {}^{\bullet}OH + OH^-\ (E^0 = +0.38\ \text{V}\ \textit{vs.}\ \text{NHE}) \quad (10)$$

$$2H^+ + 2e^- \rightarrow H_2\ (E^0 = +0.695\ \text{V}\ \textit{vs.}\ \text{NHE}) \quad (11)$$

Y. Wang *et al.* developed a novel cathode by directly growing NiFe-layered double hydroxide (LDH) on carbon paper for the electrochemical treatment of polyvinyl chloride (PVC) MPs[68] (Fig. 5a). The system operates through an electrochemical Fenton (EC-Fenton) pathway, where the Fe^{3+}/Fe^{2+} cycle activates H_2O_2 to generate $^{\bullet}OH$ radicals. In the LDH lattice, rapid electron transfer across M–O–M bonds enhances the Fe redox cycle, while abundant cation vacancies improve H_2O_2 selectivity. The degradation mechanism involves direct dechlorination of PVC driven by the applied cathodic potential, coupled with chain scission primarily induced by $^{\bullet}OH$ oxidation. Under a potential of −0.7 V *vs.* Ag/AgCl and an O_2 flow of 40 mL min^{-1}, the system achieved approximately 30% weight loss of PVC MPs within 6 h (Table 5). Lin *et al.* fabricated an FeS_2/carbon felt cathode for the EC-Fenton treatment of polyethylene terephthalate (PET) MPs.[69] With the addition of 2 mM persulfate, the cathode facilitated the reduction of both H_2O_2 and persulfate, producing to $^{\bullet}OH$ and $^{\bullet}SO_4^-$ radicals that enabled 91% decomposition of 0.1 g L^{-1} PET MPs within 12 h. Degradation proceeded through three main pathways: ester bond cleavage forming aromatic intermediates, oxidation of chain ends to carboxylic acids, and radical-induced intramolecular reactions producing terephthalic acid and other oxidized fragments. Nonetheless, the study did not provide experimental evidence to confirm the involvement of the classical Fenton pathway, as the electrochemical system alone can activate H_2O_2 and persulfate. No evidence was provided to verify the Fe(II)/Fe(III) redox cycling, and no experiments were conducted to determine the optimized operating potential or current density. Miao *et al.* employed an electrochemical Fenton-like process using a TiO_2/carbon cathode for the degradation of polyvinyl chloride MPs.[70] The mechanism involves Ti^{3+} reacting with O_2 to generate $^{\bullet}OH$ radicals while being oxidized to Ti^{4+}, which is subsequently reduced back to Ti^{3+} under the applied potential. At −0.7 V *vs.* Ag/AgCl, the system achieved 56% degradation of MPs within 6 h. However, its practical applicability remains limited, as the requirement of elevated temperature (100 °C) and continuous oxygen supply (40 mL min^{-1}) significantly increases the energy demand. Moreover, the involvement of the Ti^{3+}/Ti^{4+} cycle was not conclusively demonstrated, as the reported results only verified the generation of $^{\bullet}OH$ species at the cathode. Chen *et al.* developed a photoelectrocatalytic microreactor that integrates photocatalysis, EC processes, and microfluidics for the treatment of polystyrene nanoplastics. The microfluidic system enables precise control of multiphase flow and fine adjustment of the photoelectro-Fenton reaction. In this system, the cathode composed of MOF-derived α-Fe_2O_3 utilizes photoexcited electrons to accelerate the reduction of Fe^{3+} to Fe^{2+}, thereby enhancing the Fenton reaction for H_2O_2 activation and $^{\bullet}OH$ generation. Under an applied voltage of 1.2 V and solar irradiation of 0.12 W cm^{-2}, with a flow rate of 0.05 mL min^{-1}, the reactor achieved over 84% decomposition of PS NPs. Despite this efficiency, scaling up remains a major challenge, as the limited throughput and processing capacity hinder direct application in real water treatment systems.

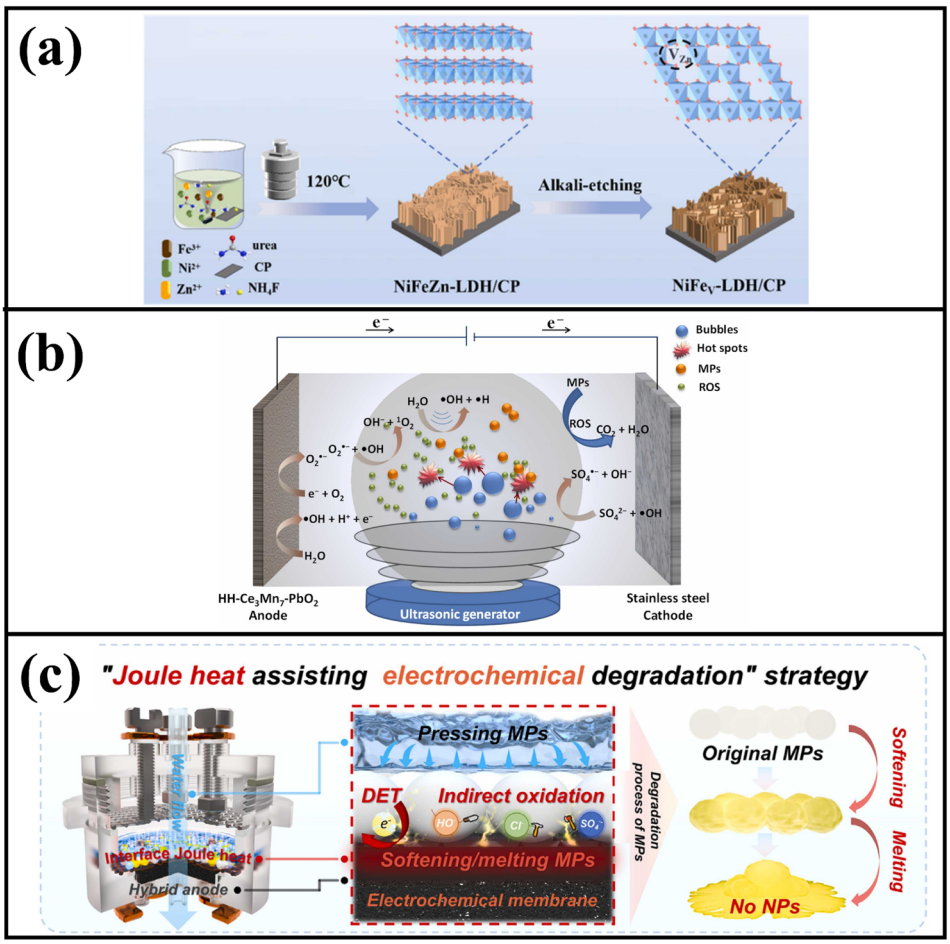

Fig. 5 Synthesis route of the NiFe-LDH/C cathode for electro-Fenton decomposition of PVC microplastics[68] (a), schematic illustration of the ultrasound-assisted electrochemical system employing a Ce_3Mn_7-PbO_2 anode for PVC microplastic degradation[71] (b), and representation of an electrochemical membrane reactor with a Ti/Sb-SnO_2/C felt membrane anode highlighting the Joule heating effect[72] (c). Adapted from ref. 68, Copyright (2025), and,[72] Copyright (2024) with permission from Elsevier. Reprinted from ref. 71, Copyright (2025) with permission from Elsevier.

In electrochemical water treatment, the anode contributes to pollutant removal through direct electron transfer or by generating $^{\bullet}OH$ from water oxidation (eqn (12)). However, efficiency is often limited by the competing oxygen evolution reaction (OER) (eqn (13)), which consumes current without degrading contaminants. Non-active anodes such as boron-doped diamond (BDD), PbO_2, and SnO_2 mitigate this issue by exhibiting high OER overpotential, favoring the accumulation of physisorbed $^{\bullet}OH$ that readily oxidizes pollutants. In contrast, active anodes like IrO_2 and RuO_2 strongly chemisorb oxygen intermediates to form surface oxides (M=O), which promote oxygen release rather than pollutant degradation.

$$H_2O \rightarrow {}^{\bullet}OH + H^+ + e^- \ (E^0 = +2.7 \text{ V } \textit{vs.} \text{ NHE}) \quad (12)$$

$$2H_2O \rightarrow O_2 + 4H^+ + 4e^- \ (E^0 = +1.23 \text{ V } \textit{vs.} \text{ NHE}) \quad (13)$$

Several studies have employed BDD as an inert anode for NMP treatment,[27,74–77] owing to its high O_2 evolution overpotential, low background current, strong stability, and efficient $^{\bullet}OH$ generation *via* water electrolysis. X. Liu *et al.* compared electrochemical systems using three different anodes for the degradation of polyvinyl chloride and polystyrene MPs.[27] Among them, the BDD anode exhibited the highest OER potential (2.08 V *vs.* SCE) and the strongest $^{\bullet}OH$ generation, achieving 54% removal of 0.1 g L^{-1} PVC MPs. The faster degradation of PVC relative to PS was attributed to its greater hydrophilicity, which enhances interaction with $^{\bullet}OH$ and adsorption onto the BDD surface. The Na_2SO_4 electrolyte contributed to the degradation process by anodic oxidation, producing $^{\bullet}SO_4^-$ radicals that acted synergistically with $^{\bullet}OH$ in MP decomposition. The PVC degradation mainly involves chain scission and progressive dechlorination, producing chlorinated fragments that undergo further cleavage, rearrangement, and radical oxidation. Hydroxyl radical attack promotes the formation of oxygenated intermediates, including aromatic and alkene compounds, which are subsequently oxidized into smaller molecules and ultimately mineralized to CO_2 and H_2O. J. Lu *et al.* (2022) investigated the degradation of polystyrene MPs using a BDD felt anode with sodium dodecyl sulfate (SDS) as an additive.[77] In this system, SDS (0.5 g L^{-1}) served as a precursor for $^{\bullet}SO_4^-$ radicals, with additional dosing every 3 h

Table 5 Overview of the recent studies using electrochemical-based processes for MNP treatment

System	NMPs (conc., shape, size)	Operational conditions	Removal efficiency and degradation rate	References
Cathodic processes				
EC system (NiFe-LDH/C paper cathode)	Polyvinyl chloride MPs (0.1 g L^{-1})	Anode: Graphite Cathode: NiFe-LDH/C Electrolyte Na_2SO_4 dose: 0.05 M O_2: 40 mL min^{-1} pH 7.2 Temperature: 75 °C Fixed potential: −0.7 V *vs.* Ag/AgCl Time: 6 h	Weight loss: 30%	68
EC system (FeS_2/C felt cathode) + persulfate	Polyethylene terephthalate MPs (0.1 g L^{-1})	Anode: BDD Cathode: FeS_2/C felt Electrolyte Na_2SO_4 dose: 0.05 M pH 3 Persulfate dose: 2 mM Temperature: 25 °C Fixed current: 1 a Time: 12 h	Weight loss: 91%	69
EC system (TiO_2/C cathode)	Polyvinyl chloride MPs (0.1 g L^{-1})	Anode: Graphite Cathode: TiO_2/C Electrolyte Na_2SO_4 dose: 0.05 M O_2: 40 mL min^{-1} pH 9 Temperature: 100 °C Fixed potential: −0.7 V *vs.* Ag/AgCl Time: 6 h	Weight loss: 56%	70
Micro EC system (MOF-derived α-Fe_2O_3 cathode) + solar light	Polystyrene nanoplastics (25 mg L^{-1})	Anode Cathode: MOF-derived α-Fe_2O_3 Electrolyte Na_2SO_4 dose: 0.05 M H_2O_2: 0.5 M Xenon lamp (120 mW cm^{-2}) pH 2 Bias voltage: 1.2 V Time: 36 s Flux: 50 μL min^{-1}	Weight loss: 84%	73
Anodic processes				
EC system (BDD anode)	Polyvinyl chloride MPs (0.1 g L^{-1}) Polystyrene MPs (0.1 g L^{-1})	Anode: BDD Cathode: Stainless steel Electrolyte Na_2SO_4 dose: 0.12 M pH 7 Temperature: 25 °C Current density: mA cm^{-2} Time: 6 h	Weight loss: 54% Weight loss: 37%	27
EC system (BDD anode)	Polystyrene MPs (0.06 g L^{-1}, 1.0 μm)	Anode: BDD Cathode: Stainless steel Electrolyte Na_2SO_4 dose: 0.02 M pH 6 Temperature: 25 °C Current density: 60 A m^{-2} Time: 5 h	Weight loss: 59%	74
EC system (BDD anode)	Polyethylene terephthalate MPs (0.1 g L^{-1}, 25–38 μm)	Anode: BDD Cathode: Ti Electrolyte Na_2SO_4 dose: 0.03 M synthetic water salt: 35% salinity pH 6–7 Current intensity: 2 a Time: 2 h	Weight loss: 95%	75

Table 5 (*Contd.*)

System	NMPs (conc., shape, size)	Operational conditions	Removal efficiency and degradation rate	References
EC system (BDD anode) PEC system (TiO_2 photoanode) + light	Polyethylene terephthalate MPs (1 g L^{-1}, 250 μm)	Anode: Si/BDD Cathode: Stainless steel Electrolyte $NaClO_4$ dose: 0.1 M Current density: 2.5 mA cm^{-2} Time: 8 days Photoanode: Nanotubular TiO_2 Cathode: Platinised Ti grid Xenon lamp (300 W) Electrolyte $NaClO_4$ dose: 0.1 M Current density: 0.1 mA cm^{-2} Time: 8 days	Weight loss: 10.2% Weight loss: 7%	76
EC system (BDD anode) + sodium dodecyl sulfate (SDS)	Polystyrene MPs (2 g L^{-1})	Anode: BDD felt Cathode: Pt Electrolyte Na_2SO_4 dose: 0.2 M Temperature: 25 °C Current density: 30 mA cm^{-2} Time: 72 h SDS dose: 0.5 g L^{-1}	Weight loss: 40%	77
EC system (Ti/SnO_2-Sb_2O_3/CeO_2-PbO_2 anode)	Polyvinyl chloride MPs (0.1 g L^{-1})	Anode: Ti/SnO_2-Sb_2O_3/CeO_2-PbO_2 Cathode: Stainless steel Electrolyte Na_2SO_4 dose: 0.09 M H 11 Temperature: 100 °C Current density: 60 mA cm^{-2} Time: 6 h	Weight loss: 39%	78
EC system (Ti/Co-Sb-SnO_2/La anode)	Polystyrene MPs (1 g L^{-1})	Anode: Ti/Co-Sb-SnO_2/La Cathode: Ti mesh Electrolyte Na_2SO_4 dose: 0.18 M Current density:107 mA cm^{-2} pH 7 Time: 3 h	Weight loss: 28%	79
EC system (Ti/SnO_2/Nb_2O_5 anode)	Polystyrene MPs (10 mg L^{-1}, 25 μm)	Anode: Ti/SnO_2/Nb_2O_5 Cathode: Ti/Pt Electrolyte NaCl dose: 2 g L^{-1} Current density: 5.8 mA cm^{-2} pH 7 Time: 6 h	Weight loss: 35%	80
EC system (CNT-PbO_2 anode) + UV light + persulfate	Polyvinyl chloride MPs (0.05 g L^{-1})	Anode: CNT-PbO_2 Cathode: stainless steel Electrolyte Na_2SO_4 dose: 0.05 M pH 9 Temperature: 90 °C Current density: 120 mA cm^{-2} PMS dose: 0.08 g L^{-1} Time: 0.5 h	Weight loss: 37%	81
Ec system (Ce_3Mn_7-PbO_2 anode) + ultrasonication	Polyvinyl chloride MPs (0.1 g L^{-1})	Anode: Ce_3Mn_7-PbO_2 Cathode: stainless steel Ultrasonication: 40 kHz, 600 W Electrolyte Na_2SO_4 dose: 0.05 M Current density: 40 mA cm^{-2} Time: 6 h	Weight loss: 72%	71
EC membrane system (Ti/Sb-SnO_2/C felt membrane anode)	Polyethylene MPs (0.8 g L^{-1})	Anode: Ti/Sb-SnO_2/C felt Cathode: mesh titanium Electrolyte NaCl dose: 0.2 M Temperature (near anode): 66 °C Current density: 20 mA cm^{-2} Time: 5 h	Weight loss: 99%	72

to maintain a steady concentration of 0.2 g L^{-1} under a current density of 30 mA cm^{-2}. The presence of SDS markedly improved the removal efficiency, achieving degradation rates 1.4–2.3 times higher than BDD electrolysis alone after long reaction process of 72 h. This enhancement was linked to two effects, the facilitation of persulfate activation with the generation of additional oxidants and the better dispersion of MPs in solution, which increased adsorption of reactive species by reducing surface hydrophobicity.

Sb, Sn, Pb, and Nb are favored in anode design because they combine stability, conductivity, and high OER overpotential, allowing them to efficiently generate reactive species. Building on these advantages, various modifications and dopants have been explored to further enhance their activity and durability.[78–80] Ning *et al.* studied doping CeO_2 on PbO_2 anode in the EC oxidation of polyvinyl chloride MPs.[78] CeO_2 incorporation into PbO_2 refined β-PbO_2 grains, enhanced active site density, and raised the OER potential from 1.80 to 1.91 V *vs.* SCE. Consequently, the CeO_2-PbO_2 anode achieved 39% MP weight loss after 6 h, markedly higher than the 22% obtained with pure PbO_2. To enhance applicability, subsequent studies are recommended to alleviate the harsh operational requirements of 100 °C and pH 11. Zheng *et al.* investigated the use of a cobalt interlayer to enhance the durability of SnO_2-based anodes during the EC degradation of polystyrene MPs.[79] While the presence of Co diminished the electrode's capacity to adsorb MPs and generate $^{\bullet}OH$ radicals, resulting in lower degradation efficiency compared to the undoped electrode, it offered notable advantages. Specifically, the Co layer reduced electrode resistance, increased current efficiency, and extended the service life to 245 h, representing a significant improvement in stability. Greater care is required in the discussion of the cyclic voltammetry spectra, since improper interpretation of peak positions, current densities, or scan-rate dependence can result in misleading conclusions about the redox behavior and catalytic mechanism. Nhan *et al.* enhanced the EC degradation of polystyrene MPs by tailoring anode morphology.[80] Using surfactant F127 during the synthesis of SnO_2/Nb_2O_5 created a mesoporous structure with enlarged surface area and abundant active sites, which improved pollutant adsorption and interaction with hydroxyl radicals. As a result, the mesoporous electrode achieved 35% removal of 0.01 g L^{-1} MPs in 6 h, far outperforming the non-templated counterpart. A limitation of this system is the high potential for trihalomethane formation due to the reaction of free chlorine, generated from the NaCl electrolyte, with organic pollutants.

Other studies have widely explored hybrid systems that integrate EC processes with other water treatment methods to overcome limitations. Huang *et al.* activated persulfate by combining UV light and EC system containing CNT-PbO_2 anode for the degradation of polyvinyl chloride MPs.[81] Persulfate can be activated both by anodic $^{\bullet}OH$ and cathodic electron transfer to yield $^{\bullet}SO_4^-$ radicals, which enhanced the process and resulted in 37% microplastic weight loss within 0.5 h of treatment. The contribution of UV irradiation to persulfate activation and overall system efficiency remains unclear, and the potential influence of CNT doping on improving PbO_2 performance has yet to be addressed. Duan *et al.* developed a Ce_3Mn_7-PbO_2 anode coupled with ultrasonication for the electrochemical degradation of polyvinyl chloride MPs.[71] The Ce^{4+}/Ce^{3+} redox couple promoted oxidative activity, while MnO_2 contributed strong catalytic properties. Surfactant modification increased the anode's hydrophobicity, reducing $^{\bullet}OH$ adsorption and thereby enhancing electrocatalytic performance. Ultrasonication further intensified $^{\bullet}OH$ interactions with MPs and facilitated the formation of additional radicals (Fig. 5b). With these improvements, the system achieved 72% MP weight loss, compared to only 25% with the unmodified PbO_2 anode. Shao *et al.* reported a hybrid approach combining electrochemical oxidation, Joule heating, and membrane filtration for the degradation of polyethylene MPs.[72] A Ti/Sb-SnO_2/C anode was fabricated in a membrane configuration to simultaneously filter MPs during treatment. The carbon felt, with its rough and porous structure, created non-uniform current distribution and high interfacial resistance, leading to localized hotspots that melted MPs and enhanced their direct oxidation (Fig. 5c). This system achieved 99% MP weight loss within 5 h while effectively suppressing the formation of secondary nanoparticles.

In summary, electrochemical oxidation represents a promising AOP for NMP removal, offering direct oxidation pathways, the generation of diverse reactive species, and the potential for integration with complementary technologies such as membrane filtration,[72] sonication,[71] photocatalysis,[76] and Fenton-based processes.[69] Considerable efforts have focused on enhancing electrode performance through morphological tailoring, increased surface area, hydrophobicity,[71] and incorporation of conductive additives such as CNTs[81] and MOF-derived materials,[73] as well as through the design of innovative reactors like microfluidic system.[73] The studies have also emphasized the identification of degradation intermediates using advanced analytical techniques (TOC,[27] fluorescence spectroscopy,[73] HPLC-MS, UPLC-Q-Orbitrap MS,[77] and PY-GC-MS[79]) and the evaluation of their toxicity and environmental impacts, for example *via* seed germination,[72] *Vibrio fischeri* inhibition,[77] and prediction of toxicity from determined structure of intermediates.[81] However, several limitations remain to be addressed in current studies. Degradation efficiency of NMPs is often assessed primarily through weight loss, which relies heavily on membrane filtration and may not fully capture transformation pathways. Many systems also require harsh operating conditions, including extended treatment times, extreme pH, or high temperature. Investigations using two-electrode configurations are constrained by poor potential control, lower efficiency, and limited mechanistic insight. In addition, electrode leakage is a critical issue that has frequently been overlooked. While integrating EC processes with other technologies can enhance overall performance, it also introduces greater complexity and higher operational costs. Future research should focus more on assessing electrode stability, including leakage analysis and EC characterization (*e.g.*, lifetime evaluation, Tafel measurements[71]) to achieve a balance between efficiency and durability. Careful assessment of energy demand and overall operational costs is also essential for advancing practical applications.[79] The effects of salts and

electrolytes need to be studied more carefully, not only as radical precursors but also regarding their post-treatment impacts, such as the possible formation of disinfection by-products like trihalomethanes when NaCl is employed.[80] In addition, computational approaches (*e.g.*, density functional theory[68]) should be utilized to elucidate the electronic properties of electrodes and their interaction mechanisms with NMPs.

6. Challenges and future perspectives

AOPs have demonstrated considerable potential for the degradation of NMPs, however, their large-scale and practical implementation is still restricted by several technique-specific limitations. Ozonation-based AOPs appear promising for the removal of NMPs although important technological and safety concerns persist. One major drawback is the rapid decomposition of ozone in aqueous media, which reduces oxidation efficiency. In addition, the assessment of NMP treatment performance is often affected by methodological inconsistencies, including subjective microscopic observations, filtration-related bias, and the use of TOC measurements that may not accurately reflect NMP mineralization. Furthermore, several studies have reported that oxidation products formed during treatment may still pose ecological risks, such as negative effects on plant germination. Photocatalytic systems also face practical challenges. The separation of catalyst particles from plastic residues remains difficult, and recovery commonly relies on filtration procedures. Many reported processes require relatively harsh operational conditions, including extreme pH, elevated temperature, or prolonged reaction times. Incomplete NMP mineralization can result in intermediate by-products, and catalyst leaching may occur, raising concerns regarding long-term stability and environmental safety. Fenton-based approaches, including heterogeneous and piezo-assisted variants, have improved certain limitations of conventional Fenton chemistry but still present notable constraints. Performance evaluation criteria are not standardized among studies, and mechanistic investigations are often limited by restricted access to advanced analytical techniques. In addition, research efforts have largely concentrated on commonly studied polymers such as polystyrene, while more resistant plastic types remain insufficiently investigated. Emerging modifications, such as bacteria-assisted or microwave-enhanced Fenton systems, may enhance NMP degradation but are typically associated with high energy demand and operational costs, which may hinder practical application. Electrochemical oxidation provides multiple oxidative pathways and strong oxidation capacity although several issues remain. In many cases, NMP degradation efficiency is estimated primarily through weight-loss measurements, which provide limited insight into mineralization and reaction mechanisms. Some electrochemical systems operate only under severe operating conditions, and the frequent use of two-electrode configurations restricts precise potential control, reducing efficiency and mechanistic understanding. Electrode stability is another concern, as leakage or material deterioration is often insufficiently examined. Although coupling electrochemical oxidation with other treatment methods can enhance NMP removal performance, such hybrid systems also increase operational complexity and cost. The potential toxicity of by-products generated during AOP treatment of MNPs has been investigated using both experimental bioassays and computational approaches. Phytotoxicity is often evaluated through seed germination and early growth tests using plants such as peas or mung beans, where indicators including germination rate, germination index, and seedling vigor are monitored. Aquatic toxicity is further examined using microbial and algal assays, such as acute toxicity tests with Vibrio fischeri, algal growth inhibition studies, and antibacterial tests involving *Escherichia coli*. In parallel, computational tools such as the Toxicity Estimation Software Tool (TEST) are employed to predict parameters such as oral LD_{50} and mutagenicity of degradation intermediates. Most studies report a reduction in toxicity after treatment, indicating that oxidative processes can transform harmful compounds into less toxic species. Nevertheless, complete or near-complete mineralization is generally recommended, as residual intermediates may still pose potential ecological risks if discharged into the environment.

Further progress in the application of AOPs for the treatment of NMPs will require the development of standardized and reliable evaluation protocols. Such protocols should be supported by advanced analytical methods and the use of closed experimental systems that enable more accurate quantification of degradation and mineralization. For instance, closed reactors coupled with alkaline trapping solutions to capture CO_2 generated during ozonation can significantly improve the reliability of mineralization assessments. Comprehensive characterization techniques, including HPLC, Py-GC/MS, GC-TOF-MS, ^{1}H NMR, and XPS, should be employed more systematically to elucidate degradation pathways and identify transformation products. In addition, emerging detection approaches, such as metal-labeling strategies combined with high-sensitivity measurements, together with computational modeling, can provide deeper insight into catalyst–polymer interactions and assist in predicting the potential toxicity of intermediate species. From a practical perspective, successful implementation will depend on the development of catalysts and electrodes that are stable, reusable, and effective under environmentally relevant conditions, while minimizing leakage, chemical consumption, energy demand, and overall production and operational costs. The design of novel photocatalysts, for example layered double hydroxides doped with high-valence metals capable of activating oxidants such as hydrogen peroxide or persulfate under light irradiation, represents a promising route for generating highly reactive oxygen species and enhancing NMP degradation. Heterogeneous Fenton systems have also shown encouraging performance, particularly when combined with piezo- or photo-assisted activation under light and ultrasound, which can alleviate some of the strongs of conventional Fenton and photo-Fenton processes, such as iron sludge generation and the need for strongly acidic conditions. Another promising strategy involves immobilizing photocatalysts on floating or high-surface-area substrates, such as porous chitin sponges, cellulose-based aerogels, or glass fibers,

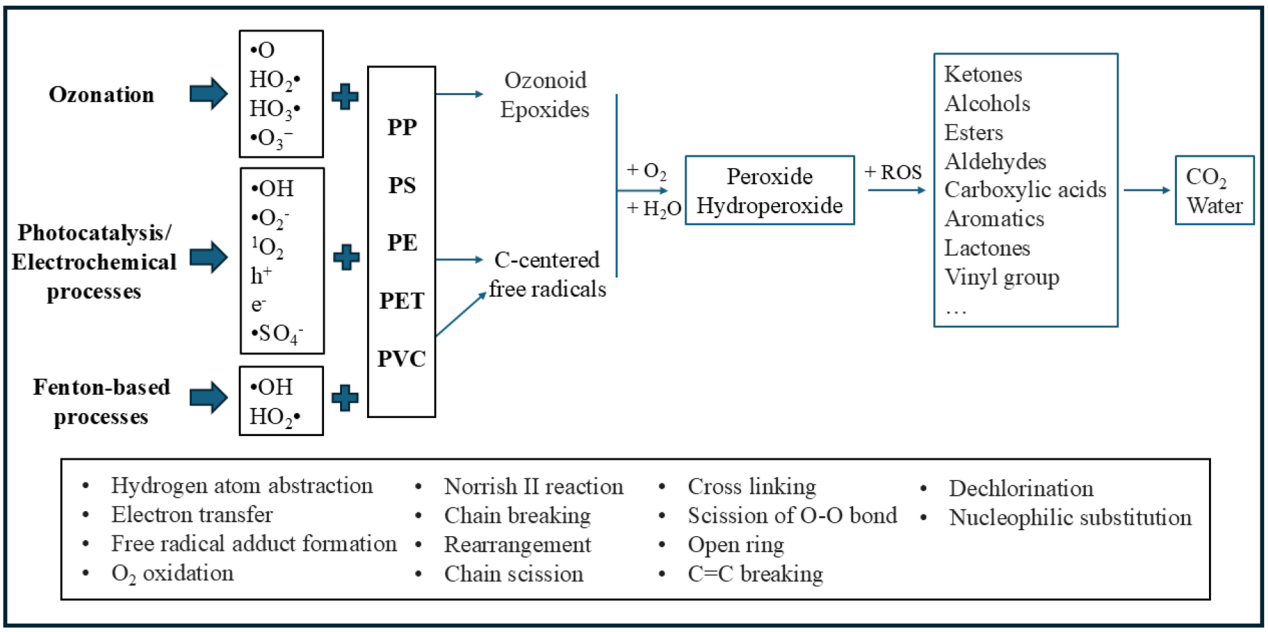

Fig. 6 Degradation pathways and the principal reactions involved in the AOP-based treatment of NMPs.

under continuous-flow operation, facilitating catalyst recovery and improving environmental compatibility. Electrochemical oxidation can be further strengthened by coupling with complementary processes, including membrane filtration, sonication, photocatalysis, or Fenton-based systems, to provide multiple oxidation pathways for effective NMP removal. Future efforts should prioritize improving electrode performance through morphological engineering, increasing surface area and hydrophobicity, and incorporating conductive additives such as carbon nanotubes or MOF-derived materials, as well as through the development of innovative reactor configurations, including microfluidic designs. At the same time, greater attention should be given to electrode durability, including leakage evaluation and electrochemical characterization (*e.g.*, lifetime testing and Tafel analysis), to achieve an optimal balance between activity and stability. Computational chemistry and theoretical modeling should also play a larger role in future studies by clarifying electronic structures and catalytic mechanisms, thereby guiding the rational design of materials with improved activity for NMP degradation. Extending the treatment duration or process should be considered to improve the complete mineralization of MNPs, thereby preventing the persistence of organic residues that may pose ecological risks and increase the need for additional treatment. Fig. 6 summarizes the degradation pathways and the principal reactions involved in the AOP-based treatment of NMPs.

Moreover, broader validation in real wastewater matrices and investigations involving polymer types beyond polystyrene are essential. Pilot-scale trials in drinking water or wastewater treatment facilities would be particularly valuable for assessing the scalability of laboratory findings and for evaluating operational parameters such as flow rate, reactor configuration, and transport behavior of NMPs. Equally important is the identification and assessment of by-products, including potentially harmful compounds originating from salts, supporting electrolytes, or partially oxidized polymers. Ultimately, the combination of AOPs with complementary or post-treatment processes, supported by cost-effective materials, advanced characterization, and computationally guided design, will be critical for translating laboratory-scale successes into scalable, sustainable, and safe technologies for the remediation of NMPs.

7. Conclusions

This review summarizes recent advances in AOP-based technologies for NMP degradation, focusing on ozonation, photocatalysis, Fenton processes, and EC oxidation. Research has largely emphasized optimizing conditions, clarifying mechanisms, and assessing intermediates, with growing attention to integrated systems that enhance performance.

Ozonation benefits from coupling with ultrasound, UV, or catalysts but is limited by ozone instability and energy costs, performing better than chlorination but less effectively than wet oxidation. Photocatalysis is a promising AOP for water treatment, but its use for NMPs remains constrained by low efficiency, high energy demand, and challenges in catalyst recovery. Advances such as heterojunctions, metal doping, composites, and oxidant activation have improved performance, while immobilization on support (*e.g.*, sponges, aerogels, fibers, or membranes) offers reuse but still faces issues like pH dependence and fragmentation. Recent studies highlight multifunctional applications, including co-removal of other pollutants or hydrogen production, supported by advanced analytical tools and computational modeling to better understand mechanisms and assess toxicity. Fenton-based processes hold promise for NMP degradation but show variable performance. Conventional systems achieve limited oxidation, while photo-assisted Fenton improves efficiency *via* light-driven

radical generation. Heterogeneous catalysts broaden operating conditions and enhance recovery but remain energy-intensive and mechanistically unclear. Emerging self-Fenton and bio-Fenton approaches are innovative yet constrained by high costs, long durations, and poor scalability. EC oxidation is a promising method for NMP removal, utilizing cathodic generation of H_2O_2 and hydroxyl radicals and anodic production of strong oxidants. Improved electrode designs, such as LDHs, carbon composites, and doped metal oxides, have enhanced charge transfer, radical production, and stability, while hybrid systems with sonication, addition of oxidants, or membranes further increase efficiency. Nonetheless, challenges remain, including reliance on weight-loss assessments, harsh conditions, limited mechanistic clarity in two-electrode setups, electrode leakage, and high energy demand.

Overall, while AOPs show strong potential for NMP remediation, their practical deployment requires standardized evaluation, better mechanistic understanding, improved electrode and catalyst stability, and energy-efficient, scalable designs to achieve safe and sustainable applications.

Author contributions

Thi Ngoc Bao Dung: writing (original draft), investigation, visualization. Thi Thanh Huyen Nguyen: writing (original draft), Quang Viet Ly: conceptualization, writing (review & editing), Hui Lin Ong: writing (original draft), Hai Bang Truong: writing (review & editing), project administration, supervision, validation.

Conflicts of interest

There are no conflicts of interest to declare.

Data availability

No primary research results, software or code have been included and no new data were generated or analysed as part of this review.

Supplementary information (SI) is available. See DOI: https://doi.org/10.1039/d5ra09364c.

References

1 H. Najahi, M. Banni, M. Nakad, R. Abboud, J. C. Assaf, L. Operato, M. Belhassen, L. Gomes and W. Hamd, *J. Hazard. Mater. Adv.*, 2025, **18**, 100667.
2 R. Kumar, A. Verma, A. Shome, R. Sinha, S. Sinha, P. K. Jha, R. Kumar, P. Kumar, Shubham, S. Das, P. Sharma and P. V. V. Prasad, *Sustainability*, 2021, **13**, 9963.
3 International Union for Conservation of Nature (IUCN), Plastic Pollution: Issues Brief, 2023.
4 N. F. Mendez, V. Sharma, M. Valsecchi, V. Pai, J. K. Lee, L. S. Schadler, A. J. Müller, S. Watson-Sanders, M. Dadmun, G. Kumaraswamy and S. K. Kumar, *Nat. Commun.*, 2025, **16**, 1–11.
5 M. Mousazadehgavan, S. Khademi, A. M. Naeini, I. Yoosefdoost, V. Vashisht, M. Hashemi, M. Manouchehri and K. Hashim, *J. Water Process Eng.*, 2024, **67**, 106159.
6 H. D. Chaudhary, G. Shah, U. Bhatt, H. Singh and V. Soni, *npj Emerg. Contam.*, 2025, **1**, 1–22.
7 A. I. Osman, M. Hosny, A. S. Eltaweil, S. Omar, A. M. Elgarahy, M. Farghali, P. S. Yap, Y. S. Wu, S. Nagandran, K. Batumalaie, S. C. B. Gopinath, O. D. John, M. Sekar, T. Saikia, P. Karunanithi, M. H. M. Hatta and K. A. Akinyede, *Environ. Chem. Lett.*, 2023, **21**, 2129–2169.
8 A. A. Mohd Ali, A. A. Khalid, N. I. Abd Razak, N. S. Mohd Maulana, N. S. Roslan, R. S. B. Razmi, W. M. A. Wan Ruseli, Y. S. Ibrahim, M. Jaafar, R. Shahrudin, K. Ismail and S. T. Anuar, *Water Emerg. Contam. Nanoplastics*, 2024, **3**, 12.
9 A. F. R. M. Ramsperger, E. Bergamaschi, M. Panizzolo, I. Fenoglio, F. Barbero, R. Peters, A. Undas, S. Purker, B. Giese, C. R. Lalyer, A. Tamargo, M. V. Moreno-Arribas, H. P. Grossart, D. Kühnel, J. Dietrich, F. Paulsen, A. K. Afanou, S. Zienolddiny-Narui, S. Eriksen Hammer, T. Kringlen Ervik, P. Graff, B. C. Brinchmann, K. C. Nordby, H. Wallin, M. Nassi, F. Benetti, M. Zanella, J. Brehm, H. Kress, M. G. J. Löder and C. Laforsch, *NanoImpact*, 2023, **29**, 100441.
10 T. Habumugisha, Z. Zhang, C. Uwizewe, C. Yan, J. C. Ndayishimiye, A. Rehman and X. Zhang, *Ecotoxicol. Environ. Saf.*, 2024, **278**, 116426.
11 R. K. Sharma, U. Kumari and S. Kumar, *Cureus*, 2024, **16**(5), e60712.
12 H. Kye, J. Kim, S. Ju, J. Lee, C. Lim and Y. Yoon, *Heliyon*, 2023, **9**, e14359.
13 S. Cunsolo, J. Williams, M. Hale, D. S. Read and F. Couceiro, *Anal. Bioanal. Chem.*, 2021, **413**, 3789–3799.
14 Y. Xu, Q. Ou, X. Wang, F. Hou, P. Li, J. P. van der Hoek and G. Liu, *Environ. Sci. Technol.*, 2023, **57**, 3114–3123.
15 Y. Li, C. Zhang, Z. Tian, X. Cai and B. Guan, *J. Hazard. Mater.*, 2024, **463**, 132933.
16 N. J. van Eck and L. Waltman, *Scientometrics*, 2010, **84**, 523–538.
17 K. Shahzad, A. Hasan, S. K. Hussain Naqvi, S. Parveen, A. Hussain, K. C. Ko and S. H. Park, *Chemosphere*, 2025, **370**, 143936.
18 A. Verma, G. Sharma, A. Kumar, P. Dhiman, G. T. Mola, A. Shan and C. Si, *Chemosphere*, 2024, **352**, 141365.
19 A. K. Badawi, R. Hasan and B. Ismail, *RSC Adv.*, 2025, **15**, 25256–25273.
20 Y. Mao, Z. Hu, H. Li, H. Zheng, S. Yang, W. Yu, B. Tang, H. Yang, R. He, W. Guo, K. Ye, A. Yang and S. Zhang, *Environ. Pollut.*, 2024, **349**, 123863.
21 K. Chabi, J. Li, C. Ye, C. Kiki, X. Xiao, X. Li, L. Guo, M. Gad, M. Feng and X. Yu, *Sci. Total Environ.*, 2024, **912**, 169074.
22 S. K. Kolluru and V. K. Raja, *Water Cycle*, 2025, **6**, 126–150.
23 Z. Lin, X. Hu, H. Lin, G. Yu, L. Shen, W. Yu, B. Li, L. Zhao and M. Ying, *Chem. Eng. J.*, 2025, **520**, 166183.
24 A. Solanki, V. Sharma, P. Sharma and D. Kumar, *J. Ind. Eng. Chem.*, 2025, **153**, 94–107.

25 M. Z. Gulzar, G. Liu, B. Yousaf, M. Imran, M. Arif, M. Nauman, M. I. S. Haider, B. Sattar, R. Safeer, S. Ijaz and R. Liu, *J. Water Process Eng.*, 2025, **74**, 107809.
26 L. D. Abo, M. Jayakumar, A. S. Jeyapaul, M. Rangaraju, H. A. Areti and A. Assefa Adugna, *Environ. Adv.*, 2025, **20**, 100638.
27 X. Liu, L. Qiu, Y. Bai, X. Zeng, Z. Zhao, X. Long, H. Bao, Y. Zhao, H. Wang, Q. Yan and S. Man, *J. Environ. Chem. Eng.*, 2025, **13**, 116686.
28 C. Solís-Balbín, D. Sol, A. Laca, A. Laca and M. Díaz, *J. Water Process Eng.*, 2023, **51**, 103456.
29 R. Zafar, S. Y. Park and C. G. Kim, *Environ. Eng. Res.*, 2020, **26**, 200412.
30 J. Wang and H. Chen, *Sci. Total Environ.*, 2020, **704**, 135249.
31 G. Pulido-Reyes, L. Magherini, C. Bianco, R. Sethi, U. von Gunten, R. Kaegi and D. M. Mitrano, *J. Hazard. Mater.*, 2022, **436**, 129011.
32 E. Topkaya, A. Arslan, M. Isgoren, M. Sezer and S. Veli, *Chem. Eng. Sci.*, 2025, **306**, 121287.
33 H. Hidayaturrahman and T. G. Lee, *Mar. Pollut. Bull.*, 2019, **146**, 696–702.
34 Y. Li, J. Li, J. Ding, Z. Song, B. Yang, C. Zhang and B. Guan, *Chem. Eng. J.*, 2022, **427**, 131690.
35 A. Pattanateeradetch, C. Sakulthaew, Y. T. Lin, A. Watcharenwong, A. Žgajnar Gotvajn, Y. C. Chen, Q. Xu and C. Chokejaroenrat, *J. Water Process Eng.*, 2025, **69**, 106800.
36 J. Hu, F. Y. Lim and J. Hu, *Sci. Total Environ.*, 2023, **866**, 161290.
37 Y. Li, C. Zhang, C. Shen, G. Jiang and B. Guan, *Environ. Res.*, 2023, **220**, 115220.
38 J. Nieto-Sandoval, R. Ammar and C. Sans, *Chem. Eng. J. Adv.*, 2024, **19**, 100621.
39 J. Hu and J. Hu, *Chemosphere*, 2024, **349**, 140839.
40 D. Zhu and Q. Zhou, *Environ. Nanotechnol. Monit. Manag.*, 2019, **12**, 100255.
41 J. Jeyaraj, V. Baskaralingam, T. Stalin and I. Muthuvel, *Environ. Res.*, 2023, **233**, 116366.
42 X. Zhang, M. Zhang, C. Luo, Y. Li, L. Zhang, C. Li, X. Zhang, J. Liao and W. Zhou, *Appl. Catal. B-Environ.*, 2025, **371**, 125288.
43 C. Cao, L. Lin, Q. Qiu, J. Wang, H. Lin, Q. Qian, Q. Chen and W. Zhou, *J. Colloid Interface Sci.*, 2025, **700**, 138490.
44 J. Jeyavani, K. A. Al-Ghanim, M. Govindarajan, G. Malafaia and B. Vaseeharan, *J. Contam. Hydrol.*, 2024, **267**, 104436.
45 X. Liu, Z. Yang, H. Liu, Y. Li and G. Zhang, *J. Hazard. Mater.*, 2024, **480**, 136080.
46 Y. Luo, H. Zheng, X. Li, F. Li, H. Tang and X. She, *Acta Phys.-Chim. Sin.*, 2025, **41**, 100052.
47 A. D. Lopis, K. S. Choudhari, R. Sai, Sudarshana, K. S. Kanakikodi, S. P. Maradur and S. D. Kulkarni, *Mater. Res. Bull.*, 2024, **176**, 112836.
48 W. Biao, N. Awanis Hashim, M. F. Bin Rabuni, O. Lide and A. Ullah, *Sep. Purif. Technol.*, 2025, **356**, 129929.
49 Z. Meng, C. Sun, C. Wang, Z. Wang, S. Deng and H. Yang, *Appl. Surf. Sci.*, 2025, **711**, 164104.
50 R. Montenegro, Z. González, A. Rodríguez, C. Canovi, P. Pozzi, C. Siligardi and E. I. Cedillo-González, *J. Environ. Manage.*, 2025, **389**, 126015.
51 A. Uheida, H. G. Mejía, M. Abdel-Rehim, W. Hamd and J. Dutta, *J. Hazard. Mater.*, 2021, **406**, 124299.
52 F. Wu, H. Yu, F. Chang, K. Tang, J. Xu, Y. Dou and W. Zhang, *Sep. Purif. Technol.*, 2025, **364**, 132394.
53 T. Poerio, C. Lavorato, A. Severino, B. Russo, R. Molinari, P. Argurio and A. Figoli, *J. Environ. Chem. Eng.*, 2024, **12**, 113310.
54 B. Cao, S. Wan, Y. Wang, H. Guo, M. Ou and Q. Zhong, *J. Colloid Interface Sci.*, 2022, **605**, 311–319.
55 X. Wang, Z. Zhu, J. Jiang, R. Li and J. Xiong, *Chemosphere*, 2023, **337**, 139206.
56 Y. Liu, Q. Zeng, S. Ning, Y. Gan, T. Fujita, Y. Wei, X. Wang and D. Zeng, *J. Solid State Chem.*, 2024, **333**, 124645.
57 F. Wu, J. Qin, B. Yin, Y. Zhang, C. Li, Y. Dou, C. Hélix-Nielsen and W. Zhang, *Appl. Catal. B-Environ.*, 2025, **365**, 124853.
58 D. Ortiz, M. Munoz, J. Nieto-Sandoval, C. Romera-Castillo, Z. M. de Pedro and J. A. Casas, *Chemosphere*, 2022, **309**, 136809.
59 B. Liu, Q. Jiang, Z. Qiu, L. Liu, R. Wei, X. Zhang and H. Xu, *Chemosphere*, 2022, **298**, 134220.
60 C. di Luca, J. Garcia, D. Ortiz, M. Munoz, J. Carbajo, Z. M. de Pedro and J. A. Casas, *J. Environ. Chem. Eng.*, 2023, **11**, 110755.
61 C. di Luca, J. Garcia, M. Munoz, L. Fasce, Z. M. de Pedro and J. A. Casas, *Appl. Catal. B-Environ.*, 2025, **362**, 124751.
62 M. Wu, R. Wang, L. Miao, P. Sun, B. Zhou, Y. Xiong and X. Dong, *J. Colloid Interface Sci.*, 2025, **682**, 738–750.
63 W. Sun, Y. Zhou, H. Zou and G. Liu, *J. Hazard. Mater.*, 2025, **495**, 139150.
64 X. Gu, L. Li, Y. Wu and W. Dong, *J. Environ. Chem. Eng.*, 2024, **12**, 112958.
65 Y. Lu, Y. Dong, W. Liu, Q. Jin and H. Lin, *Chem. Eng. J.*, 2025, **508**, 160935.
66 Y. Yang, J. Chen, Z. Chen, Z. Yu, J. Xue, T. Luan, S. Chen and S. Zhou, *Water Res.*, 2022, **223**, 118979.
67 M. Sun, X. Huo, H. Yan, D. Ma, T. Tan, G. Zeng, L. Qin and C. Lai, *Coord. Chem. Rev.*, 2026, **546**, 217111.
68 Y. Wang, H. Zhong, Q. Xu, M. Dong, J. Yang, W. Yang, Y. Feng and Z. M. Su, *J. Hazard. Mater.*, 2025, **485**, 136797.
69 Y. Lin, Y. Zhang, Y. Wang, Y. Lv, L. Yang, Z. Chen, B. J. Ni and X. Chen, *J. Hazard. Mater.*, 2024, **478**, 135635.
70 F. Miao, Y. Liu, M. Gao, X. Yu, P. Xiao, M. Wang, S. Wang and X. Wang, *J. Hazard. Mater.*, 2020, **399**, 123023.
71 X. Duan, Z. Ning, X. Sui, S. Geng, H. Wang, C. Liu and L. Chang, *J. Environ. Chem. Eng.*, 2025, **13**, 116207.
72 D. Shao, W. Zhao, S. Ji, C. Yang, J. Zhang, R. Guo, B. Zhang, W. Lyu, J. Feng, H. Xu, W. Yan and H. Song, *Appl. Catal. B-Environ.*, 2024, **357**, 124281.
73 Q. Chen, L. Wan, H. Zhou, F. Luo, L. Lei and N. Wang, *J. Water Process Eng.*, 2023, **56**, 104343.
74 G. Falco, A. Fenti, S. Galoppo, S. Chianese, D. Musmarra, M. Cocca, S. Mallardo and P. Iovino, *J. Water Process Eng.*, 2024, **68**, 106418.

75 P. Gokul Gangadharan, A. Bharti and A. Mondal, *J. Water Process Eng.*, 2025, **76**, 108101.
76 N. Melis, M. G. Rubanu, L. Mais, M. Mascia and A. Vacca, *Electrochim. Acta*, 2025, **537**, 146905.
77 J. Lu, R. Hou, Y. Wang, L. Zhou and Y. Yuan, *Water Res.*, 2022, **226**, 119277.
78 Z. Ning, X. Duan, Y. Li, X. Zhao and L. Chang, *J. Clean. Prod.*, 2023, **432**, 139668.
79 W. Zheng, Z. Liu, B. Wang, M. Tao, H. Ji, X. Xiang, Z. Fu, L. Liao, P. Liao and R. Chen, *Sci. Total Environ.*, 2024, **922**, 171002.
80 N. T. Nhan, T. Le Luu, J. Trippel and M. Wagner, *Surf. Interfaces*, 2025, **72**, 107178.
81 J. Huang, W. Wang, T. Wu, X. Ren and X. Zhao, *RSC Adv.*, 2024, **14**, 16150–16169.